

NURail Project

NURail2015-UKY-R10-combined

The final report for NURail project: **NURail2012-UKY-R10** consists of two distinct documents.

- Section 1, 30 pages, titled “Implementation of a rail crossing condition index: Rideability Assessment”, written by Dr. Reginald Souleyrette and Dr. Teng Wang
- Section 2, 31 pages, titled “Implementation of a rail crossing condition index: Hump Crossing Evaluation”, written by Dr. Reginald Souleyrette and Dr. Teng Wang

These were completed under grant number: DTRT13-G-UTC52.



National University Rail Center - NURail
US DOT OST-R Tier 1 University Transportation Center

NURail Project ID: NURAIL2015-UKY-R10 (A)

Implementation of a rail crossing condition index:

Rideability Assessment

By

Reginald R. Souleyrette
Commonwealth Professor and Chair of Civil Engineering
University of Kentucky
souleyrette@uky.edu

Teng Wang
Post-Doctoral Associate
University of Kentucky
wangtengyilang@uky.edu

07-05-2016

Grant Number: DTRT13-G-UTC52

DISCLAIMER

Funding for this research was provided by the NURail Center, University of Illinois at Urbana - Champaign under Grant No. DTRT13-G-UTC52 of the U.S. Department of Transportation, Office of the Assistant Secretary for Research & Technology (OST-R), University Transportation Centers Program. The contents of this report reflect the views of the authors, who are responsible for the facts and the accuracy of the information presented herein. This document is disseminated under the sponsorship of the U.S. Department of Transportation's University Transportation Centers Program, in the interest of information exchange. The U.S. Government assumes no liability for the contents or use thereof.



TECHNICAL SUMMARY

Title

Implementation of a rail crossing condition index: Rideability Assessment

Introduction

Annually, over 2000 rail highway crossing crashes in the U.S. result in nearly 300 fatalities. Crossing roughness is a concern for the motoring public from a comfort and vehicle maintenance perspective, and to highway authorities from a maintenance perspective. Roughness may even increase the risk of crossing crashes. However, with 216,000 rail highway grade crossings in the US, maintenance management is a large undertaking. Crossings deteriorate over time, sometimes rapidly, and life cycle costs increase without preventive maintenance. However, while methods are available to quantify highway roughness, no method currently exists to quantitatively assess the condition of rail crossings. Because conventional inspection relies on qualitative judgment based on an inspector's perception of the crossing, effect on different vehicles and perception by other drivers is unknown. Further, roughness may be due to as-built geometry, crossing deterioration, or a combination of both. A quantifiable and extensible procedure is thus desired and is the subject of this report.

Approach and Methodology

This report presents the development of a simple, scalable, and readily deployable surface-based method of crossing evaluation. This method has the advantage of separating performance effects due to a) crossing surface condition/deterioration, and b) original/as-built design of the crossing.

This report first presents the development of a crossing roughness measure, estimated solely from a 3D point cloud and using established surface roughness parameters. Second, a crossing rideability measure is derived from smoothed 3D point cloud data and simple differentiation (smoothed rideability index). This measure of rideability is compared to field accelerometer measurements and can be used, in conjunction with functional or design classification to prioritize crossing improvements. Lastly, by subtracting the theoretical accelerations a vehicle would experience for the crossing were it in perfect condition, from field measured accelerations, a different crossing rideability index (profile-relative rideability index) is developed which can be used to prioritize crossing improvement based on condition alone.

Findings

In this report, three different quantitative crossing assessment indices are presented. The Crossing Roughness Index and the Crossing Rideability Index were both developed based on the crossing 3D point cloud only. The Crossing Roughness Index calculates the roughness due to geometric characteristics of actual crossing surface condition and profile grades of highway approaches. The Crossing Rideability Index estimates RMS of vertical accelerations as the second derivative of the

crossing vertical profile. The last, Crossing Condition Index, separates the acceleration contribution of surface condition plus vehicle response from that of original vertical curve design.

Conclusions

The Crossing Roughness Index and the Crossing Rideability Index were used to rank the performance of four different crossings and the results are compared to accelerometer measurements. Another metric, the Crossing Condition Index, is developed to separate the contributions to total acceleration from surface condition and as-built design.

Recommendations

Depending on data availability and actual application needs, single or multiple indices may be chosen to assess crossing condition. The roughness and rideability measurement and assessment methodologies developed in this report could be used to measure and monitor system assets over time, and could also be extended to other infrastructure components such as highway pavements and bridges. It is also possible that the methods and techniques developed in this research could be applied to precise 3D datasets and be useful to those analyzing long term performance of innovative rail track designs and materials, such as asphalt underlayment or tie cushioning.

Publications

Wang, Teng, "3D Infrastructure Condition Assessment for Rail Highway Applications" (2016). Chapter 6. Quantitative Crossing Assessment Indices. Theses and Dissertations--Civil Engineering. Paper 41. http://uknowledge.uky.edu/ce_etds/41

Primary Contact

Principal Investigator

Reginald R. Souleyrette
Commonwealth Professor and Chair
Civil Engineering
University of Kentucky
859-257-5309
souleyrette@uky.edu

Other Faculty and Students Involved

Teng Wang
Post-Doctoral Associate
Civil Engineering
University of Kentucky
515-441-6644
wangtengyilang@uky.edu

NURail Center

217-244-4999
nurail@illinois.edu
<http://www.nurailcenter.org/>

TABLE OF CONTENTS

LIST OF TABLES..... vii

LIST OF FIGURES viii

SECTION 1. INTRODUCTION..... 1

SECTION 2. DATA COLLECTION 1

SECTION 3. CROSSING ROUGHNESS INDEX..... 4

SECTION 4. CROSSING RIDEABILITY INDEX..... 9

SECTION 5. CROSSING CONDITION INDEX (SEPARATING THE EFFECTS OF CONDITION AND DESIGN) 13

SECTION 6. SUMMARY AND CONCLUSION 20

REFERENCES 22

LIST OF TABLES

Table 3-1 Crossing Roughness Index	6
Table 4-1 Crossing Rideability Index vs. measured accelerations at 20 MPH.....	10
Table 4-2 Crossing Rideability Index vs. measured accelerations at posted speeds.....	12
Table 5-1 Condition Index for study crossings	18

LIST OF FIGURES

Figure 2.1 Bryan Station Road crossing.	2
Figure 2.2 Briar Hill crossing.	2
Figure 2.3 Hatton Road crossing.	3
Figure 2.4 Bridgeport-Benson Road crossing.	3
Figure 3.1 Arithmetic mean height (Olympus Corporation, 2016).	4
Figure 3.2 Root mean squared height (Olympus Corporation, 2016).	5
Figure 3.3 Crossing Roughness Index rank	6
Figure 3.4 Normalized Crossing Roughness Index vs normalized field accelerations.	7
Figure 3.5 Effect of profile only	8
Figure 3.6 Differences between as-built and current surface models.	8
Figure 4.1 Actual surface vs smoothed surface.	9
Figure 4.2 Normalized accelerations at 20 MPH.	11
Figure 4.3 Normalized accelerations at posted speeds.	12
Figure 5.1 Vertical Curve Design.	13
Figure 5.2 Briar Hill Road profile and fitted vertical curve.	16
Figure 5.3 Briar Hill has a posted speed of 35 mph.	17
Figure 5.4 Two components of crossing rideability	18
Figure 5.5 General shapes of crossing profiles.	19
Figure 5.6 Bridgeport-Benson profile and fitted vertical curve.	20

SECTION 1. INTRODUCTION

Annually, over 2000 rail highway crossing crashes in the U.S. result in nearly 300 fatalities. Crossing roughness is a concern for the motoring public from a comfort and vehicle maintenance perspective, and to highway authorities from a maintenance perspective. Roughness may even increase the risk of crossing crashes. However, with 216,000 rail highway grade crossings in the US, maintenance management is a large undertaking. Crossings deteriorate over time, sometimes rapidly, and life cycle costs increase without preventive maintenance. However, while methods are available to quantify highway roughness, no method currently exists to quantitatively assess the condition of rail crossings. Because conventional inspection relies on qualitative judgment based on an inspector's perception of the crossing, effect on different vehicles and perception by other drivers is unknown. Further, roughness may be due to as-built geometry, crossing deterioration, or a combination of both. A quantifiable and extensible procedure is thus desired.

This report presents the development of a simple, scalable, and readily deployable surface-based method of crossing evaluation. This method has the advantage of separating performance effects due to a) crossing surface condition/deterioration, and b) original/as-built design of the crossing.

This report first presents the development of a crossing roughness measure, estimated solely from a 3D point cloud and using established surface roughness parameters. Second, a crossing rideability measure is derived from smoothed 3D point cloud data and simple differentiation (smoothed rideability index). This measure of rideability is compared to field accelerometer measurements and can be used, in conjunction with functional or design classification to prioritize crossing improvements. Lastly, by subtracting the theoretical accelerations a vehicle would experience for the crossing were it in perfect condition, from field measured accelerations (Wang, Souleyrette, Lau, Aboubakr, & Randerson, 2015), a different crossing rideability index (profile-relative rideability index) is developed which can be used to prioritize crossing improvement based on condition alone.

SECTION 2. DATA COLLECTION

3D data were collected for four Lexington, KY area crossings using the Optech Lynx SG1 mobile LiDAR system. Raw data were first processed to provide a bare earth model. Points related to vegetation, gates and signs were all removed to reduce the data size for computation (Wang, Souleyrette, Lau, & Xu, 2014). The processed point clouds are visualized in Figure 2.1, through Figure 2.4.

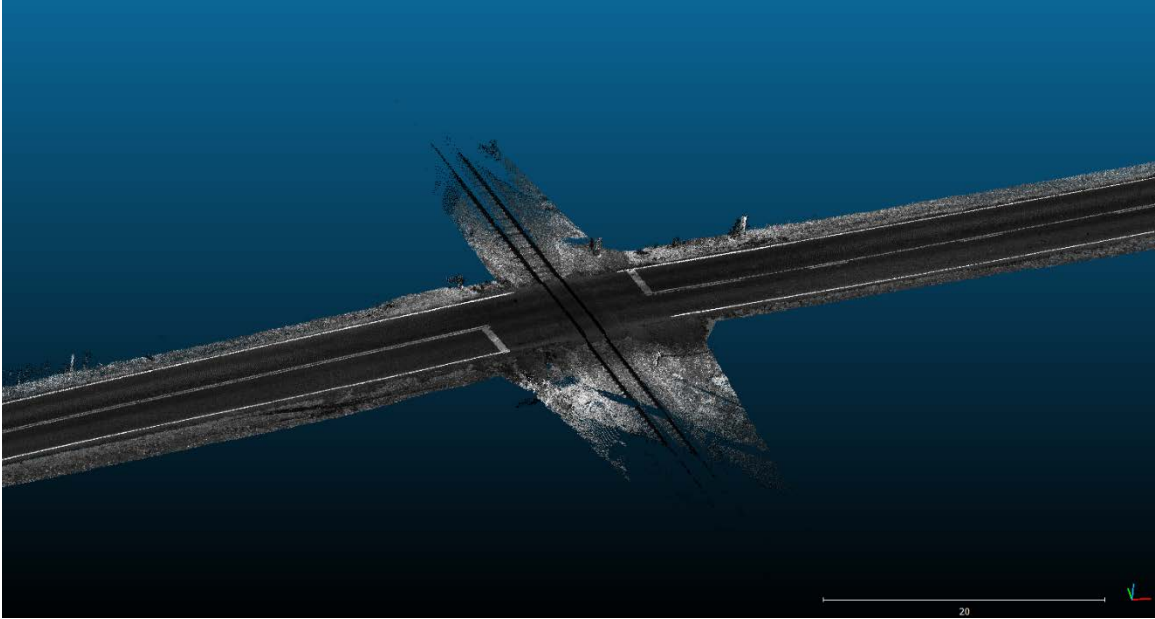


Figure 2.1 Bryan Station Road crossing.

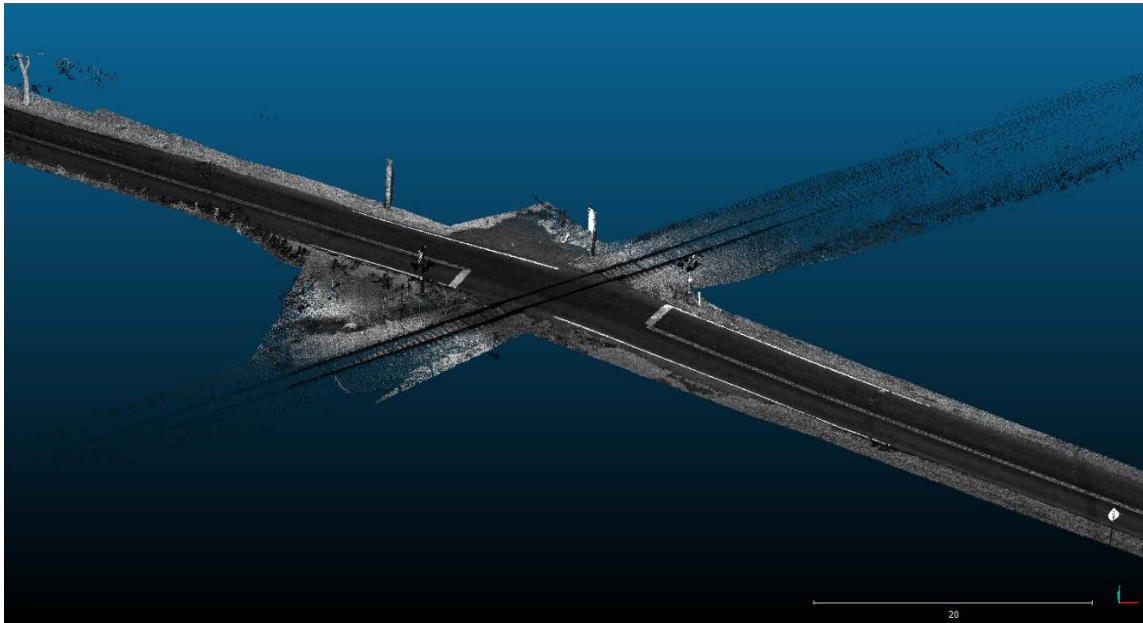


Figure 2.2 Briar Hill crossing.

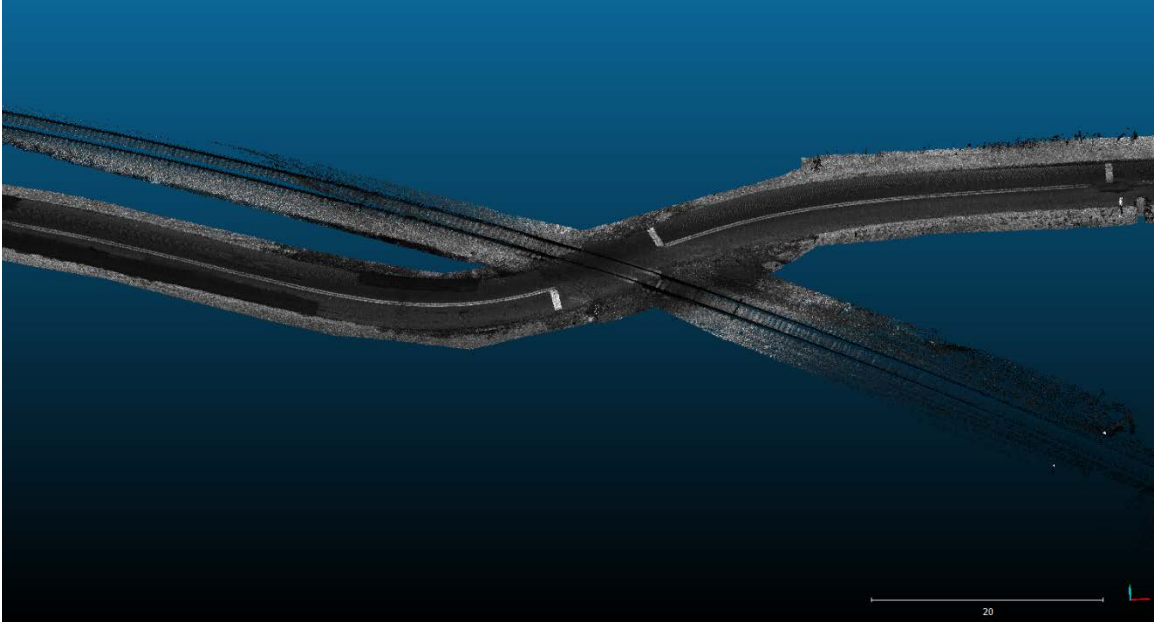


Figure 2.3 Hatton Road crossing.

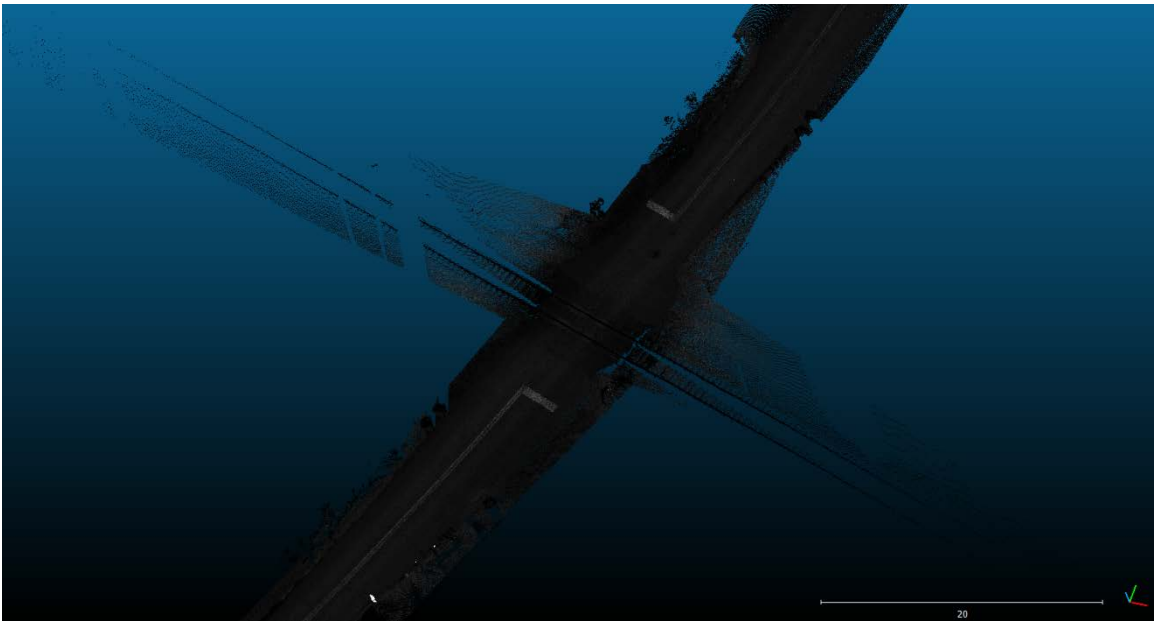


Figure 2.4 Bridgeport-Benson Road crossing.

Because the raw LiDAR data have sub-centimeter resolution, there are over two million points in each crossing data file. To reduce the size of the data file for more efficient processing, the point clouds were cropped to dimensions of 70 feet along the centerline of the highway and 20 feet in width. The intersection of the centerlines of rail and highway were used to define the center of a local coordinate system for each crossing. Further, the density of each point cloud was thinned to five inch spacing, as passenger vehicle and larger tires have at least five by five inch contact areas, and finer

deviations in surface are not likely to affect vehicle ride. This reduced the size of each point cloud from approximately two million points to just over 8,000 points—a much more manageable data set for analysis and presentation.

SECTION 3. CROSSING ROUGHNESS INDEX

Several standard measures of surface roughness are available. These measures are used for applications ranging from industrial manufactured surfaces texture (Lonardo, Trumpold, & De Chiffre, 1996) to characterization of surface deposits from volcanic eruptions (Whelley, Glaze, Calder, & Harding, 2014). Two basic measures are relevant to the current work.

First, areal arithmetic mean height (S_a) (Abouelatta, 2010) may be computed from Equation 3-1 as the average of absolute differences between a surface and its mean plane:

Equation 3-1

$$S_a = \frac{1}{MN} \sum_{j=1}^N \sum_{i=1}^M |z(x_i, y_j)|$$

Where:

M = total number of points along the X axis.

N = total number of points along the Y axis.

z = the elevation of point (xi, yj) at the XY plane.

Figure 3.1 presents a physical interpretation of this measure.

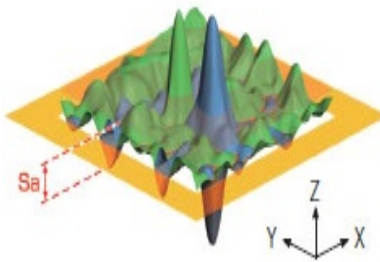


Figure 3.1 Arithmetic mean height (Olympus Corporation, 2016).

Second, areal root mean squared height (S_q) (Abouelatta, 2010) may be computed from Equation 3-2. Figure 3.2 presents a physical interpretation of this second measure. which is always greater than or equal to S_a .

Equation 3-2

$$S_q = \sqrt{\frac{1}{MN} \sum_{j=1}^N \sum_{i=1}^M z^2(x_i, y_j)}$$

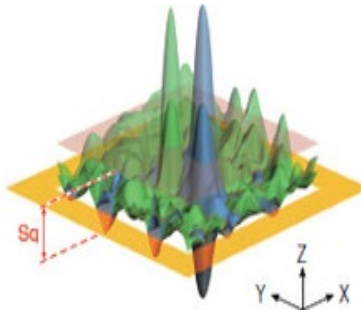


Figure 3.2 Root mean squared height (Olympus Corporation, 2016).

Both of these measures are calculated for each of the four crossings. Two surfaces are used in these computations. First, the entire 70-foot by 20-foot area is used (all 5”x5” grid cells). Next, only the approximate wheel paths of the crossings are used. For each crossing, there are four wheel paths, two in each direction. Table 3-1 presents the computed roughness indices for each crossing and each parameter for both total surface and wheel paths only. The ordered rank of crossings is the same for all measures. However, if there were significant variation (more extreme values) between wheel paths and entire surfaces (e.g., potholes, rutting, etc.), rank is more likely to be affected by choice of parameter.

Table 3-1 Crossing Roughness Index

Crossing	Entire Surface Area		Wheel path Area	
	Sa	Sq	Sa	Sq
Bryan Station	4.9	5.6	4.8	5.6
Briar Hill	7.7	9.5	7.7	9.5
Hatton	4.2	5.3	4.2	5.4
Bridgeport-Benson	5.2	6.3	5.1	6.2

Figure 3.3 shows that for the four study crossings, relative surface roughness measures are similar whether computed along the wheel path or across the entire crossing surface.

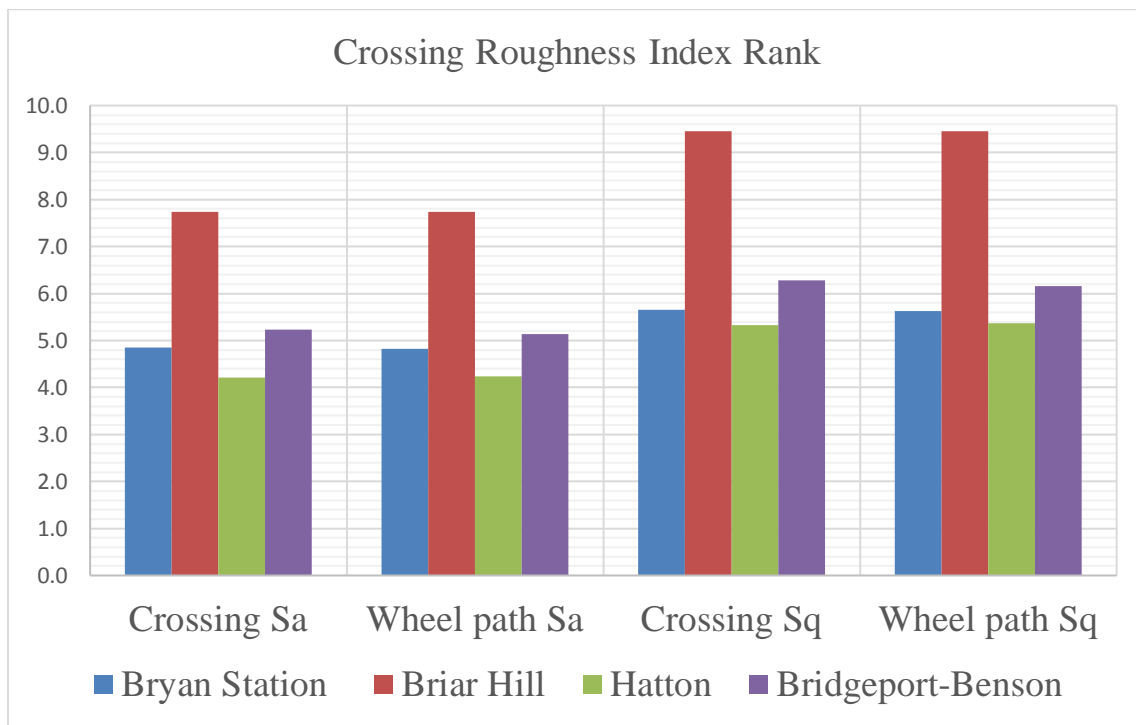


Figure 3.3 Crossing Roughness Index rank

To validate the relative measures provided by the surface roughness index, they can be normalized on a scale of 100 and compared to normalized field measured accelerations. Figure 3.4 shows there is little similarity between computed Sa and field measures of acceleration.

To explain, recall that simple computations of the Sa or Sq index makes use of a flat reference plane to determine the index. The use of such a plane limits the ability of the index to differentiate the effects of surface and profile, potentially creating absurd characterizations of smoothness. For example, Figure 3.5 illustrates a case where relative crossing “smoothness” would not be properly represented by these metrics. While Sa computed for surface A of the figure would be much greater than that computed for surface B, surface A is clearly smoother. In fact, the only cases where the use of a flat reference plane to calculate the measures would be correct, would be where both crossings had identical as-built profiles. Clearly, this is not realistic, as almost all crossings are different. This explains why Bryan Station has the lowest measured acceleration, but not the smoothest surface.

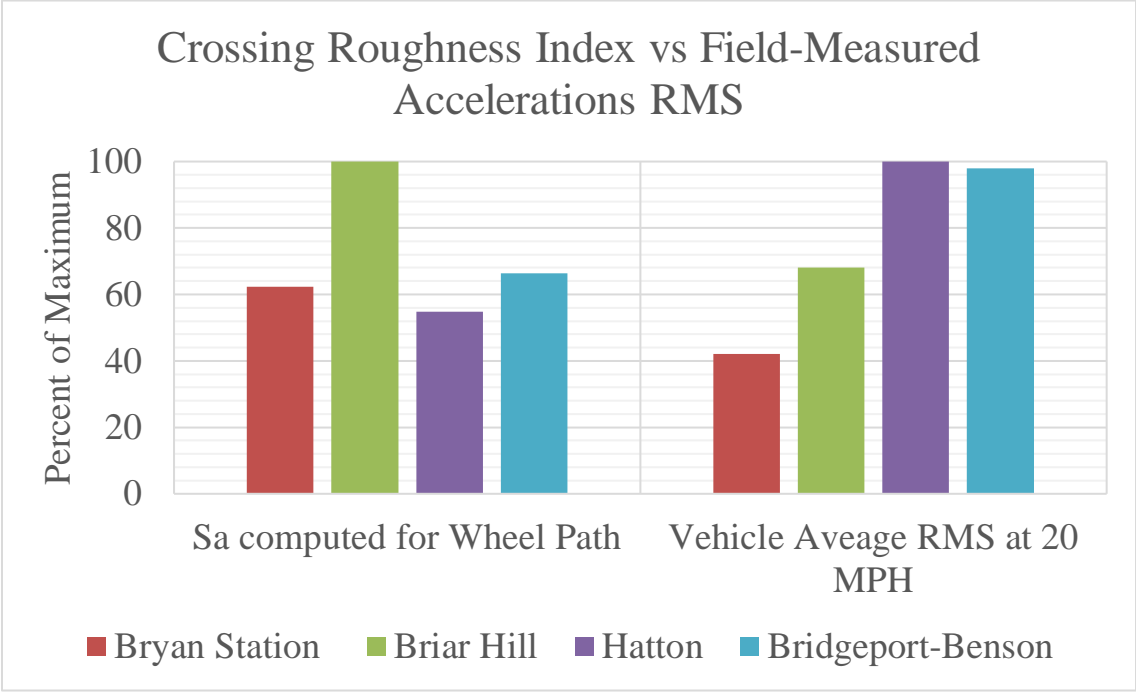
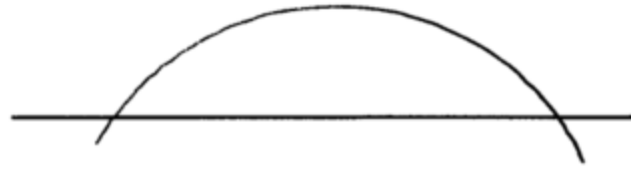
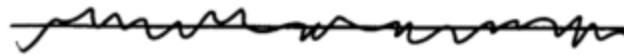


Figure 3.4 Normalized Crossing Roughness Index vs normalized field accelerations.



Crossing Profile A



Crossing Profile B

Figure 3.5 Effect of profile only

A potential solution to the problem caused by the flat plane may be to compute the metrics based on the actual surface compared to a locally-smoothed surface (a “de-noised” profile). Section 4 of this report presents an approach based on this general concept.

Another possible solution to the problem would be to calculate the metrics based on differences between as-built and current surface models (Figure 3.6). Section 5 of this report demonstrates the potential utility of such an approach.

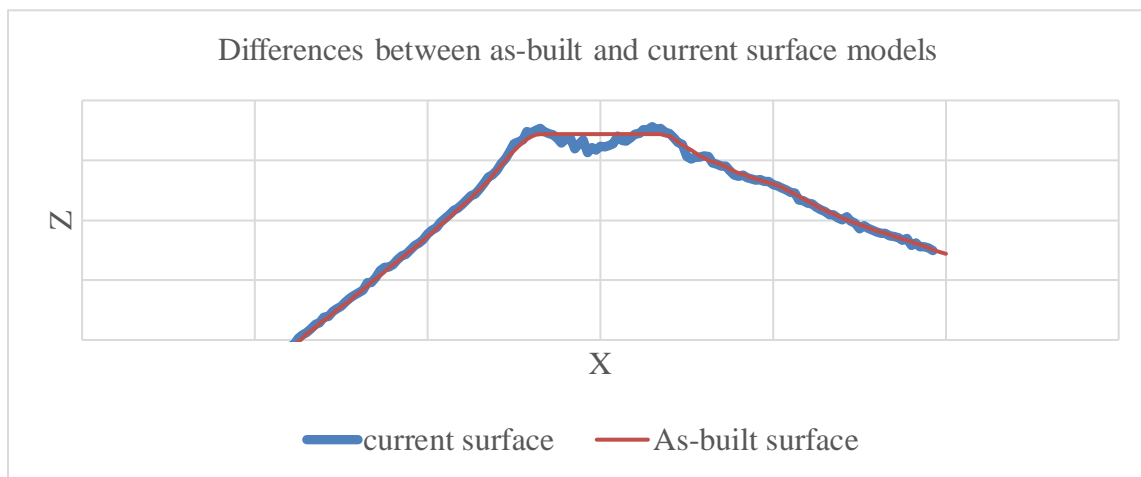


Figure 3.6 Differences between as-built and current surface models.

SECTION 4. CROSSING RIDEABILITY INDEX

The previous section developed measures which can be used to compare crossings based on surface model only, but that do not reliably predict the accelerations experienced by vehicles (rideability). This section presents a method which can be used to rank crossings with regards to their rideability as well. Predicting accurate values of acceleration is difficult (Wang, Souleyrette, Aboubakr, & Lau, 2015). However, prediction of relative accelerations is more feasible, and can be estimated using first principles of physics (vertical acceleration is the second derivative of vertical position with respect to time in the direction of travel). This can be readily computed based only upon the 3D surface model and an assumption of constant speed.

Initially, the second derivative of the sequential points on the actual surface were used to calculate accelerations. However, this resulted in exceedingly high estimates of acceleration as it would neglect the effect of vehicle suspension which smooths out the effects of small deviations. Therefore, a moving average along the surface profile was used to capture only more significant variations in surface (see Figure 4.1). A five-point moving average (20 inches) was used to compute relative accelerations in this work. Further investigations of moving average spacing could be a subject of future research.

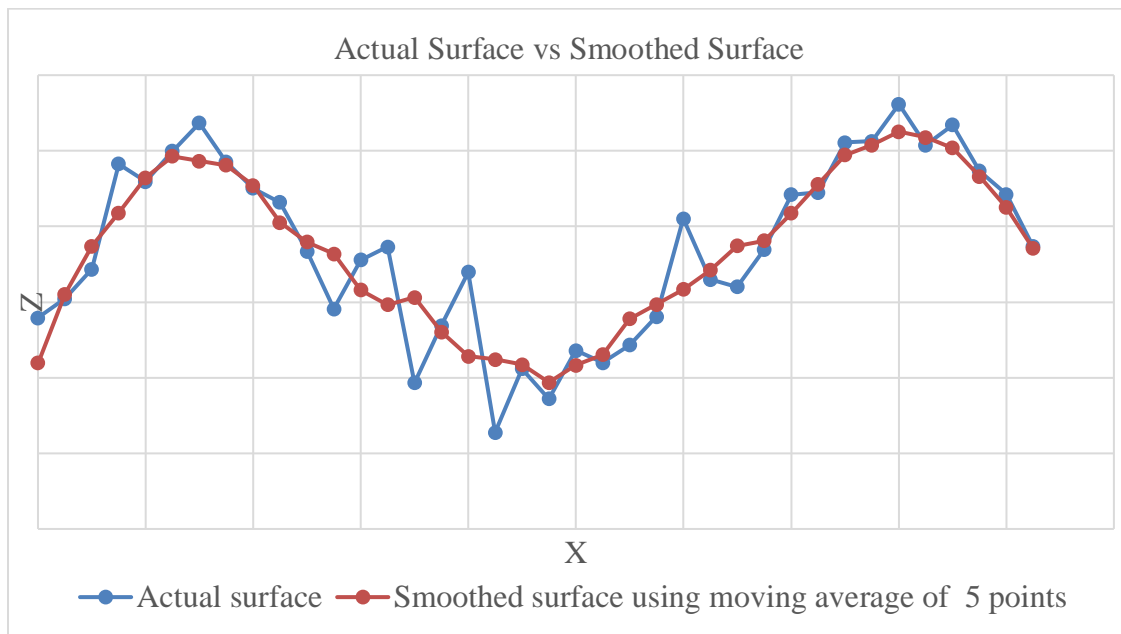


Figure 4.1 Actual surface vs smoothed surface.

In this section, computed accelerations are averaged by the root mean square method to determine a metric which can be compared to the field measured acceleration-derived RMS. This proposed metric (RMS of computed acceleration) is referred to as the “crossing rideability index.” To establish a baseline relationship between crossing rideability and actual vehicle field-measured

accelerations, the crossing rideability indices estimated by this method are compared to field readings for a common vehicle speed (20 MPH). Results are presented in Table 4-1.

There are two important observations to be made from these results. First, the accelerations predicted by the rideability index are still an order of magnitude higher than field readings. However, this is to be expected due to the damping effects of the vehicle suspension. Second, the relative ranking of crossing accelerations is closely approximated by the index. That is, the crossings with highest field readings are also those that are estimated to be highest by the index. Figure 4.2 shows the relative ratings of acceleration RMS normalized to maximum levels. For the four crossings evaluated, the Crossing Rideability Index reflects relative real-world observations.

Table 4-1 Crossing Rideability Index vs. measured accelerations at 20 MPH.

	Crossing Rideability Index (Entire Crossing Surface)	Crossing Rideability Index (Wheel path)	Accelerometer Measured Acceleration (average of all vehicles)
Bryan Station	8.5	7.9	0.42
Briar Hill	7.9	7.1	0.68
Hatton	14.2	13.4	1.00
Bridgeport-Benson	13.6	12.2	0.98

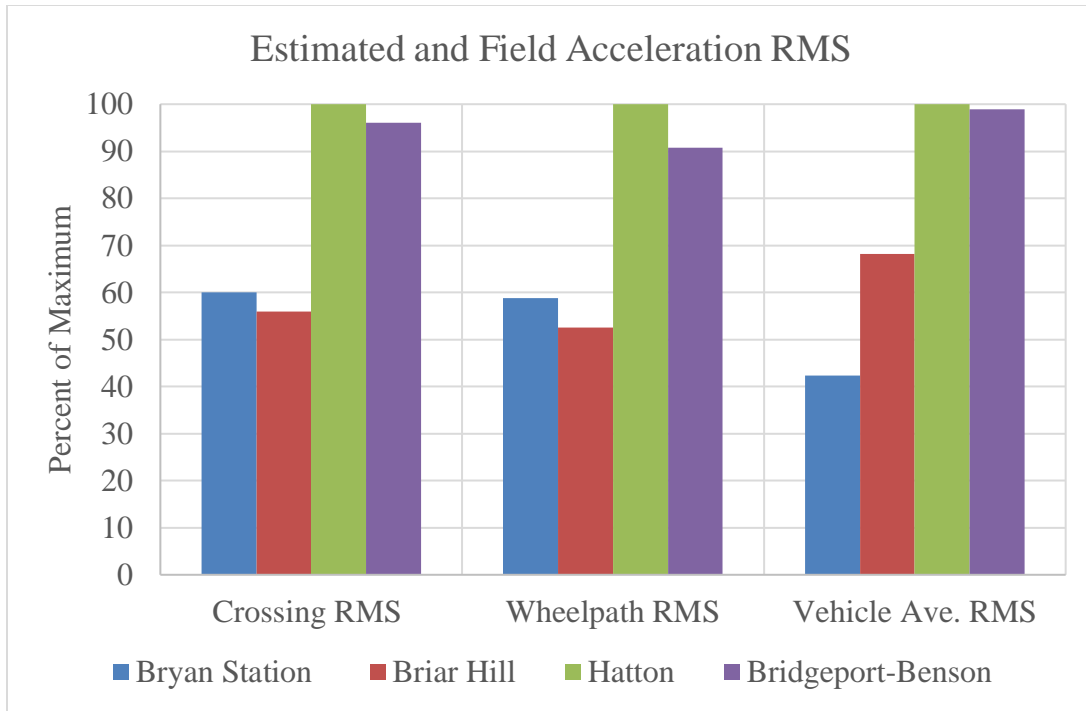


Figure 4.2 Normalized accelerations at 20 MPH.

The analysis to this point assumes a constant speed to compare crossings (in this case, 20 MPH). Generally, roads designed for mobility will have higher design speeds than those provided for access. While the public expects to slow down for railroad crossings, they also expect to be able to maintain higher speeds for higher functionally classed roads. Slowing vehicles to 20 MPH or even lower to comfortably negotiate a rail crossing on a major highway is not acceptable. Therefore, posted speed at the crossing relative to design speed of the highway should be taken into account when prioritizing improvements.

To address the importance of the crossing and therefore the practical aspects of ranking crossings for improvement, accelerations are calculated for the posted (desirable) highway speed. These accelerations are again compared to field readings as shown in Table 4-2. Again, there are two observations to be made from these results. As with the analysis of accelerations at 20 MPH, the accelerations predicted by the Crossing Rideability Index at posted speed are also an order of magnitude higher than field readings. And again, the relative ranking of crossing accelerations is closely approximated by the index. Figure 4.3 shows the relative ratings of acceleration RMS normalized to maximum levels.

Table 4-2 Crossing Rideability Index vs. measured accelerations at posted speeds.

	Crossing Rideability Index (Entire Crossing Surface)	Crossing Rideability Index (Wheel path)	Accelerometer Measured Acceleration (average of all vehicles)
Bryan Station (30mph)	19.1	17.8	0.67
Briar Hill (35mph)	24.3	21.6	1.74
Hatton (20mph)	14.2	13.4	0.99
Bridgeport-Benson (25mph)	21.3	19.1	1.09

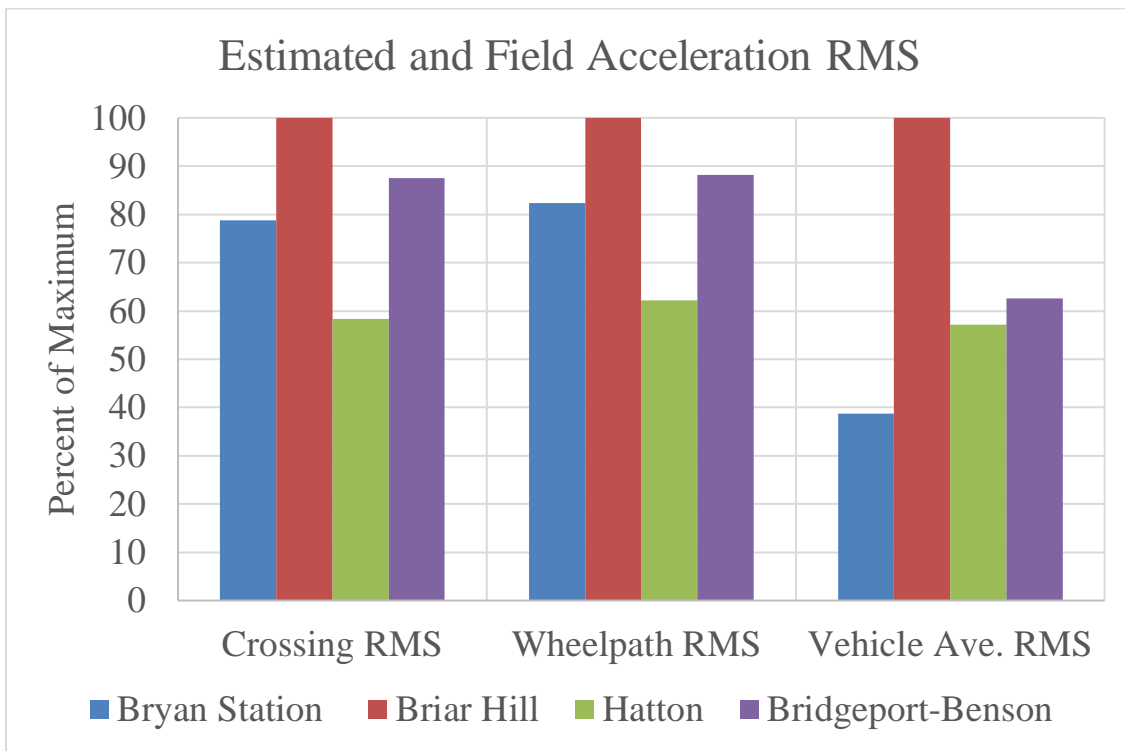


Figure 4.3 Normalized accelerations at posted speeds.

G1 and G2 = gradients of a slop in percent.

L = total length of vertical curve in feet.

E_{VPC} = elevation of VPC in feet.

When the vehicle is driven at a constant speed the following equation is obtained:

Equation 5-2 $x = vt$

Where:

t = travel time in second.

v = speed in ft/s.

Then,

Equation 5-3

$$y = \frac{G_2 - G_1}{200L} (vt)^2 + \frac{G_1}{100} (vt) + E_{VPC}$$

Taking the second derivative, one obtains:

Equation 5-4

$$a = \frac{d^2y}{dt^2} = \frac{G_2 - G_1}{100L} v^2$$

Where:

a = acceleration on the vertical direction in ft/s².

Setting “a” equal to 1.0 fps² results in:

Equation 5-5

$$L = \frac{G_2 - G_1}{100} v^2$$

When speed v is converted from ft/s into mph, Equation 1-7 becomes

Equation 5-6

$$L = \frac{G_2 - G_1}{46.5} v^2$$

Where:

L = total length of vertical curve in feet.

G_1 and G_2 = gradients of a slop in percent.

v =horizontal speed in mph

Reordering the terms produces:

Equation 5-7

$$v = \sqrt{\frac{46.5L}{G_2 - G_1}}$$

Where v is the vehicle longitudinal (speedometer) speed v and vertical acceleration is held to 1 ft/s^2 .

To demonstrate the estimation of acceleration due to as-built profile, the Briar Hill road centerline crossing profile (extracted from the 3D point cloud surface model) is plotted as shown in Figure 5.2. A hypothetical as-built crossing profile is fit to this profile by establishing VPC and VPT and best-fit tangent lines.

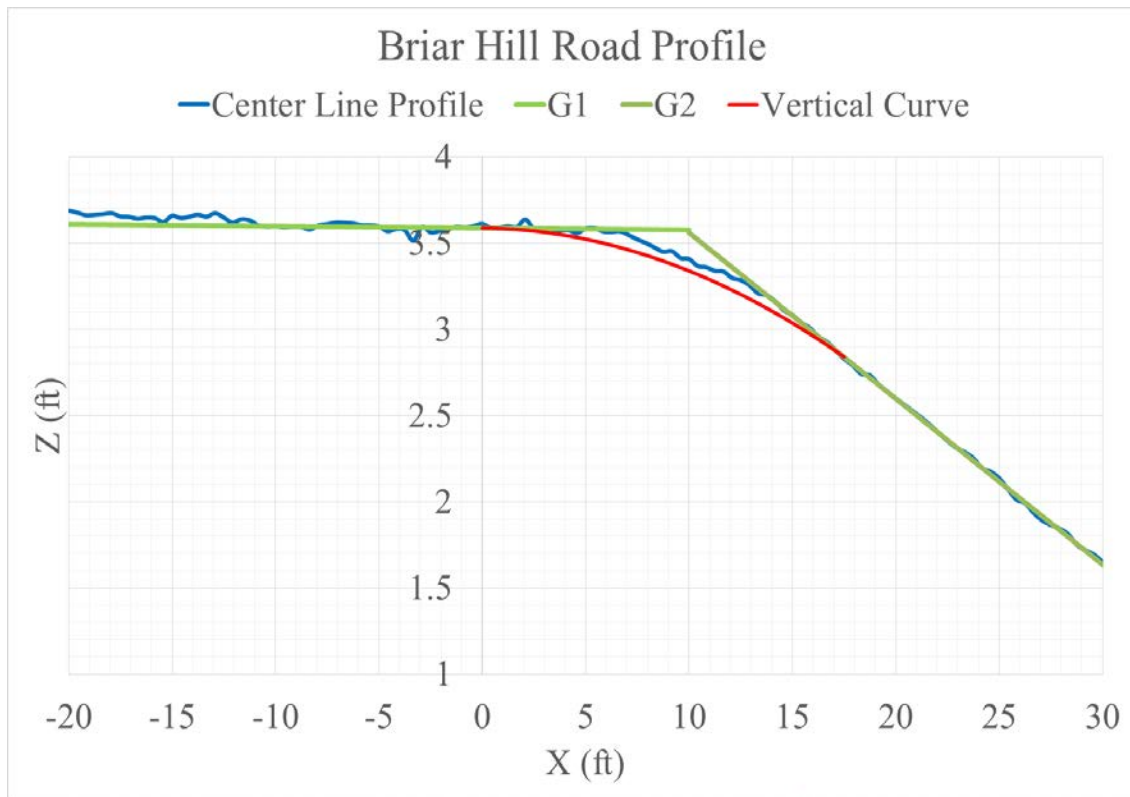


Figure 5.2 Briar Hill Road profile and fitted vertical curve.

From the plot, G1, G2 and L are measured as -0.10%, -0.96% and 17.5 feet, respectively. It is interesting to note that the length of vertical curves for this and many railroad crossings are much less than that that recommended for open road design. For example, the length of vertical curve needed to accommodate 35 mph operations at 1.0 fps^2 or 0.3 m/s^2 is 250 feet! However, in practice such long curves are not practical to construct at many locations.

It is interesting to recall the high accelerations experienced by vehicles crossing Briar Hill at the 35 mph posted speed (see Figure 5.3) suggesting that the highway agency may wish to reconsider the recommended speed at this location.



Figure 5.3 Briar Hill has a posted speed of 35 mph.

Using Equation 5-7, the speed at which a vehicle may be driven over the theoretical as-built vertical curve at Briar Hill while limiting the vertical acceleration to a comfortable 1.0 fps^2 is calculated as 9.3 mph.

From Equation 5-4, it can be seen that acceleration is proportional to the square of velocity, and thus,

Equation 5-8

$$\frac{a_1}{a_2} = \left(\frac{v_1}{v_2}\right)^2$$

Therefore, the vertical acceleration when the vehicle is driving over this curve at the 35 mph posted speed can be calculated as 14.3 fps^2 or 4.4 m/s^2 .

Based on the field-measured acceleration data, the average acceleration of all vehicles crossing Briar Hill Road at 35 mph is 7.0 m/s^2 . Clearly, most of this acceleration is caused by the vehicle negotiating the as-built profile. However, 2.6 m/s^2 of acceleration is unexplained. It is proposed that this residual is due to the surface condition of the crossing (and rail crossing surface geometry/materials), mitigated by the suspension of the vehicle. This residual may be defined as the “condition index” of the crossing. The condition index for the Briar Hill Road crossing is therefore 2.6 m/s^2 . Table 5-1 presents the condition indices calculated for the four study crossings. Figure 5.4 illustrates the two components of crossing rideability (profile-related acceleration and condition-related acceleration).

Table 5-1 Condition Index for study crossings

Crossing	Posted Speed mph	Field Measured Maximum Negative Acceleration (m/s ²)	Acceleration estimated from profile (m/s ²)	condition index (m/s ²)
Bryan Station	30	4.0	1.1	2.9
Briar Hill	35	7.0	4.4	2.6
Hatton	20	5.0	1.4	3.6
Bridgeport-Benson	25	6.0	1.7	4.3

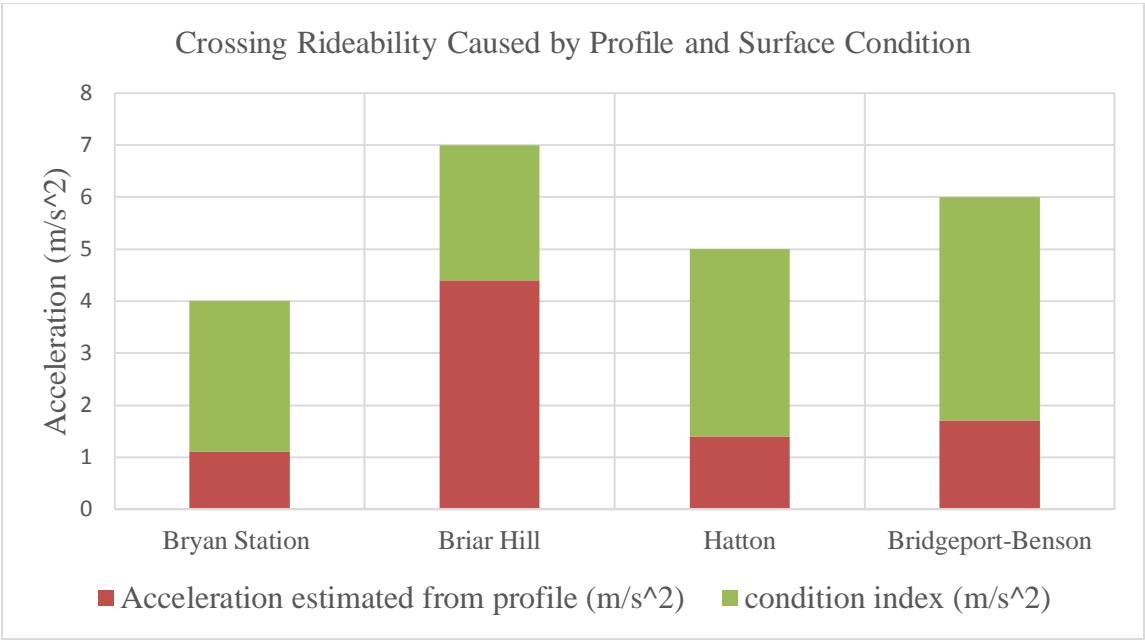


Figure 5.4 Two components of crossing rideability

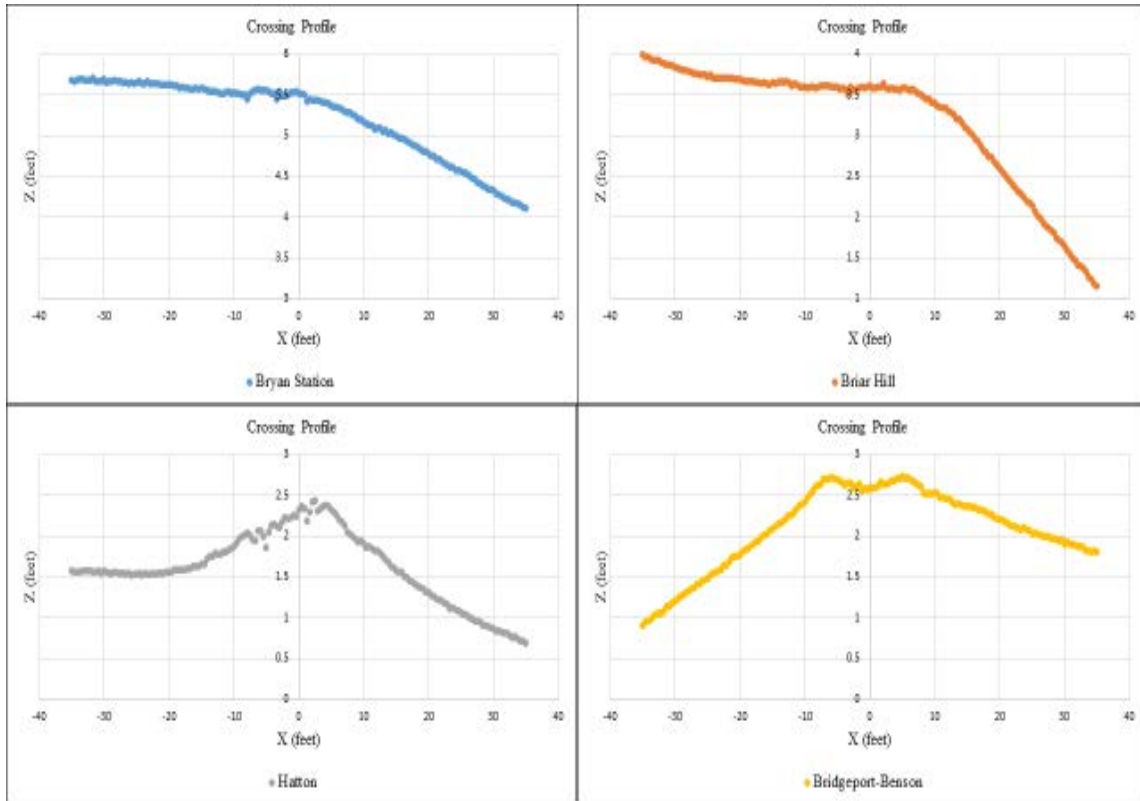


Figure 5.5 General shapes of crossing profiles.

The resulting condition indices seem consistent with the general shapes of each crossing profile (see Figure 5.5). For example, visually, Hatton Rd appears to be in the worst shape, surface-wise. However, amongst all crossings, it is clear that Bridgeport-Benson has the roughest profile.

There are several limitations of the proposed approach. These include:

- Field measured accelerations are quite variable, especially maximum accelerations (therefore, RMS was used for ranking)
- Rough condition produces both positive and negative accelerations, while profile generally will produce only positive (sag) or negative (crest) accelerations (assuming only one vertical curve in the design); as previously mentioned, crossings are not always designed, so their original profile may not be a simple vertical curve
- Complexity of vehicle response
- Unless as-built diagrams or 3D surface plots are available from the time of construction, judgment is required in the selection of points defining the as-built profile. Condition index, as defined, is sensitive to the selection of these points, especially the length of curve. For

example, at Briar Hill, changing the estimated original curve length from 17.5 to 20 changes the condition index from 2.6 to 3.2 m/s².

- A crossing may appear to have been constructed with multiple slopes/curves (see Figure 5.6, Bridgeport-Benson). However, it is unlikely that such short vertical curves were actually constructed as such, it is more likely that the curvature observed in the current condition is caused by settlement or re-lining of the track, or buildup of asphalt at road approaches.

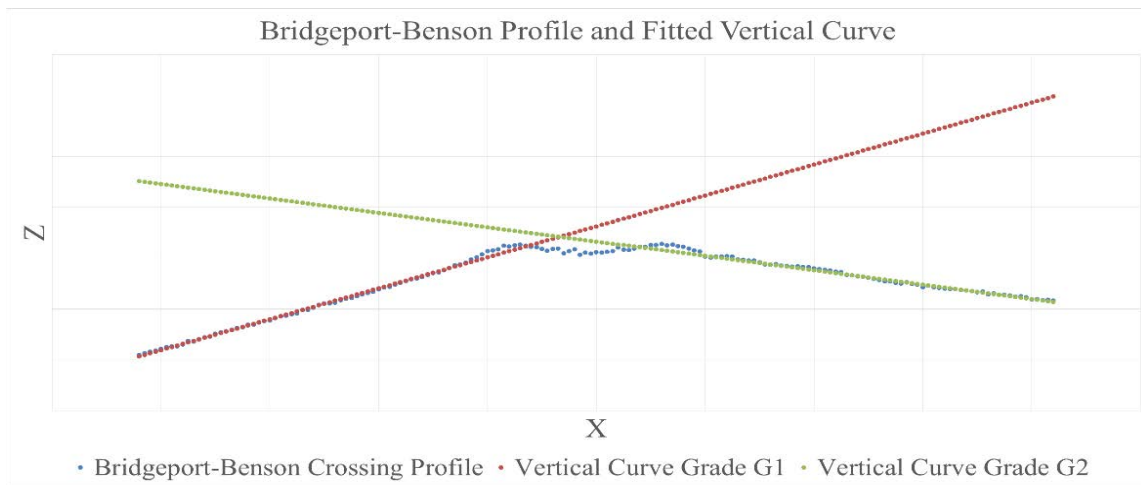


Figure 5.6 Bridgeport-Benson profile and fitted vertical curve.

SECTION 6. CONCLUSIONS AND RECOMMENDATIONS

In this report, three different quantitative crossing assessment indices were presented. The Crossing Roughness Index and the Crossing Rideability Index were both developed based on the crossing 3D point cloud only. The Crossing Roughness Index calculates the roughness due to geometric characteristics of actual crossing surface condition and profile grades of highway approaches. The Crossing Rideability Index estimates RMS of vertical accelerations as the second derivation of the crossing vertical profile. The last, Crossing Condition Index separates the acceleration contribution of surface condition plus vehicle response from that of original vertical curve design. The Crossing Roughness Index and the Crossing Rideability Index were used to rank the performances of four different crossings and the results compared to the accelerometer measurement method.

Depending on data availability and application needs, single or multiple indices may be chosen to assess crossing condition. The roughness and rideability measurement as well as assessment methodologies developed in this report may be used to measure and monitor system assets over time, and could be extended to other infrastructure components such as highway pavements and bridges. It is also possible that the methods and techniques developed in this research could be applied to precise 3D

datasets and be useful to those analyzing long term performance of innovative rail track designs and materials, such as asphalt underlayment or tie cushioning.

REFERENCES

- Abouelatta, O. B. (2010). *3D surface roughness measurement using a light sectioning vision system*. Paper presented at the Proceedings of the World Congress on Engineering, London, UK.
- Lonardo, P. M., Trumpold, H., & De Chiffre, L. (1996). Progress in 3D Surface Microtopography Characterization. *CIRP Annals - Manufacturing Technology*, 45(2), 589-598. doi:[http://dx.doi.org/10.1016/S0007-8506\(07\)60513-7](http://dx.doi.org/10.1016/S0007-8506(07)60513-7)
- Olympus Corporation. (2016). Roughness (3D) parameter (pp. Height Parameters (amplitude mean in the height direction)).
- Wang, T., Souleyrette, R. R., Aboubakr, A. K., & Lau, D. (2015). A Dynamic Model for Quantifying Rail-Highway Grade Crossing Roughness. *Journal of Transportation Safety & Security*, 00-00. doi:10.1080/19439962.2015.1048016
- Wang, T., Souleyrette, R. R., Lau, D., Aboubakr, A., & Randerson, E. (2015). *Quantifying Rail-Highway Grade Crossing Roughness: Accelerations and Dynamic Modeling*. Paper presented at the Transportation Research Board 94th Annual Meeting.
- Wang, T., Souleyrette, R. R., Lau, D., & Xu, P. (2014). *Rail Highway Grade Crossing Roughness Quantitative Measurement Using 3D Technology*. Paper presented at the 2014 Joint Rail Conference. <http://dx.doi.org/10.1115/jrc2014-3778>
- Whelley, P. L., Glaze, L. S., Calder, E. S., & Harding, D. J. (2014). LiDAR-derived surface roughness texture mapping: application to Mount St. Helens pumice plain deposit analysis. *Geoscience and Remote Sensing, IEEE Transactions on*, 52(1), 426-438.



National University Rail Center - NURail
US DOT OST-R Tier 1 University Transportation Center

NURail Project ID: NURAIL2015-UKY-R10 (B)

Implementation of a rail crossing condition index:

Hump Crossing Evaluation

By

Reginald R. Souleyrette
Commonwealth Professor and Chair of Civil Engineering
University of Kentucky
souleyrette@uky.edu

Teng Wang
Post-Doctoral Associate
University of Kentucky
wangtengyilang@uky.edu

07-05-2016

Grant Number: DTRT13-G-UTC52

DISCLAIMER

Funding for this research was provided by the NURail Center, University of Illinois at Urbana - Champaign under Grant No. DTRT13-G-UTC52 of the U.S. Department of Transportation, Office of the Assistant Secretary for Research & Technology (OST-R), University Transportation Centers Program. The contents of this report reflect the views of the authors, who are responsible for the facts and the accuracy of the information presented herein. This document is disseminated under the sponsorship of the U.S. Department of Transportation's University Transportation Centers Program, in the interest of information exchange. The U.S. Government assumes no liability for the contents or use thereof.



TECHNICAL SUMMARY

Title

Implementation of a rail crossing condition index: Hump Crossing Evaluation

Introduction

The Rail-highway grade crossing is a complex structure created to facilitate the intersection of two very different transportation modes. Due to the unique characteristics of the crossing itself and varying dynamic performance of the vehicle and train, crossings represents a potentially dangerous situation for both rail and highway users.

A hump crossing, defined as a crossing where a vehicle with low ground clearance may become high-centered or stuck, may increase the risk of crashes for both trains and automobiles. In addition to the safety implications presented by the potential of a high-centered vehicle becoming stuck on the tracks, there are operational costs associated with slowing to negotiate such a crossing, planning a trip to make sure a hump crossing will not be encountered and even more-so, the costs of diversion. Hump crossings are addressed in the design materials of agencies of the various different states. Due to the types of vehicles that are most likely to become stuck, hump crossing collisions can result in catastrophic events. Crashes at hump crossings, besides being devastating, attract public attention, as the vehicles can be vehicles designed to transport large numbers of people.

Design guidelines are available for constructing crossings in such a way as to reduce or eliminate the probability of a vehicle becoming high-centered. However, many crossings are not built to these standards. In Kentucky, assessment of hump crossings is limited. Based on an inspector's judgment, hump crossings are cataloged in a single field of the State's road inventory—a field which simply includes a yes or a no. Where crossings are assessed quantitatively (in Kentucky or elsewhere), a 2D approach is used (based on the road profile only, or, if based on a 3D pavement model, are still restricted to 2D for the vehicle). However, no methods exist to evaluate the potential impact of pavement cross section variation on all possible contact points of the vehicle and pavement. In part, the cost and difficulty of collecting 3D data has likely limited the development of tools for such analysis.

Today, 3D data are becoming widely available. Given a 3D point cloud, the distance between any two points of a crossing as well as and elevation differences between surfaces can be readily measured. Scenarios where vehicles with low ground clearance may become high-centered or hung-up on a crossing may be determined based on vehicle dimensions such as wheel base length and clearance height. Not only may such an application of 3D technology identify hump crossings, it may also be possible to quantify the severity of potential interference (some trucks "drag" their loads across) and be used to proactively improve safety at crossings.

Approach and Methodology

In this report, a method to quantify and evaluate the complex geospatial interaction between vehicles and crossings is presented. The current design guidelines for rail grade crossings, previous studies and applications of hump crossing identification and current research and application of 3D data collection for rail grade crossings are discussed. Field tests data are collected. A detailed methodology for identifying and assessing hump crossings has been developed, tested and verified with field hump crossing assessment.

Findings

This report presented the development and testing of a methodology to identify and quantify the potential severity of hump crossings. Results indicate promise for the use of 3D datasets to improve systems inventories and reduce potential risks of highway-rail collisions due to vehicles becoming stuck at crossings. With the proposed methodology, all possible contact areas between vehicle undersides and crossings can be investigated.

Conclusions

The method provides a far richer database to road managers than a simple yes/no inventory. Warning areas are identified and can be customized to any vehicle with known geometry. Once a crossing 3D point cloud is obtained, any vehicle and any wheel path can be simulated to provide results without the need for field visits and concomitant risks. Of course, the practical application of such a methodology depends on the availability of 3D data.

Recommendations

The methods presented in this report may be extended by future research into tunnel and bridge clearance, real-time warning systems, autonomous vehicles, or non-transportation applications. Refinements of the proposed approach could be to investigate the impact of dynamic forces on hump crossing conflict, incorporating aspects such as speed and suspension into the model.

Publications

Wang, Teng, "3D Infrastructure Condition Assessment For Rail Highway Applications" (2016). Chapter 7. Rail Crossing Safety: Identification and Assessment of Hump Crossings. Theses and Dissertations--Civil Engineering. Paper 41. http://uknowledge.uky.edu/ce_etds/41

Primary Contact

Principal Investigator

Reginald R. Souleyrette
Commonwealth Professor and Chair
Civil Engineering
University of Kentucky
859-257-5309
souleyrette@uky.edu

Other Faculty and Students Involved

Teng Wang
Post-Doctoral Associate
Civil Engineering
University of Kentucky
515-441-6644
wangtengyilang@uky.edu

NURail Center

217-244-4999
nurail@illinois.edu
<http://www.nurailcenter.org/>

TABLE OF CONTENTS

LIST OF TABLES..... vii

LIST OF FIGURES viii

SECTION 1. INTRODUCTION..... 1

SECTION 2. BACKGROUND 2

SECTION 3. ACQUISITION 3D DATA OF CROSSING PAVEMENT 3

SECTION 4. METHODOLOGY FOR QUANTIFYING RAIL-HIGHWAY HUMPS CROSSINGS 8

SECTION 5. ANALYSIS AND RESULTS 16

SECTION 6. VERIFICATION 19

SECTION 7. CONCLUSION AND RECOMMENDATIONS 21

REFERENCES 22

LIST OF TABLES

Table 4-1 Parameters of typical low clearance vehicles.....	11
Table 5-1 Evaluation of Railroad – Highway crossing.....	17

LIST OF FIGURES

Figure 2.1 Rail-Highway grade crossing vertical alignment (AASHTO, 2011).....	2
Figure 3.1 Crossing A: Bryan Station Road (USDOT #346839X) aerial photo.....	4
Figure 3.2 Crossing A: Bryan Station Road LiDAR point cloud.....	4
Figure 3.3 Crossing A: Bryan Station Road centerline profile.	5
Figure 3.4 Crossing B. Brannon Road crossing (USDOT # 841647U) aerial photo.	5
Figure 3.5 Crossing B. Brannon Road crossing LiDAR point cloud.	6
Figure 3.6 Crossing B. Brannon Road crossing centerline profile.....	6
Figure 3.7 Crossing C. Briar Hill Road Army Depot Road crossing (USDOT # 346849D) aerial photo.	7
Figure 3.8 Crossing C. Briar Hill Army Depot Road crossing LiDAR point cloud	7
Figure 3.9 Crossing C. Briar Hill Army Depot Road crossing centerline profile.	8
Figure 4.1 Hump crossing coordinate system (not to scale).	9
Figure 4.2 Vehicle model dimensions and coordinate system (not to scale).	10
Figure 4.3 Analysis procedure flow chart.....	12
Figure 4.4 Preprocessed 3D data of KY-57 Briar Hill Army Depot crossing.	13
Figure 4.5 Car carrier trailer.....	15
Figure 4.6 Car carrier trailer contact points at KY-57 Briar Hill Army Depot crossing.	16
Figure 5.1 Contact points on KY-57 Bryan Station crossing (A)	18
Figure 5.2 Contact points on Brannon Rd crossing (B).....	18
Figure 5.3 Contact points on KY-57 Briar Hill Army Depot (C).....	19
Figure 6.1 Field verification A.	19
Figure 6.2 Field verification B.	20
Figure 6.3 Crossing scratch marks A.....	20

Figure 6.4 Crossing scratch marks B..... 21

SECTION 1. INTRODUCTION

Quality of surface is an important aspect affecting both the safety and the performance of at-grade rail-highway crossings. A hump crossing, defined as a crossing where a vehicle with low ground clearance may become high-centered or stuck, may increase the risk of crashes for both trains and automobiles (Bauer, 1958). Crashes at hump crossings, besides being devastating, attract public attention, as the vehicles most likely to be involved are large trucks or mass transit vehicles. For example, video of a recent limousine-train crash at a hump crossing in New Paris, Indiana was posted on the Internet (StudioNoeProductions, 2015). Although in this case no one was injured, the video attracted over two million viewers and highlights the hump crossing safety issue.

Design guidelines are available for constructing crossings in such a way as to reduce or eliminate the probability of a vehicle becoming high-centered (American Railway Engineering Maintenance-of-Way Association (AREMA), 2015). However, many crossings are not built to these standards. In Kentucky, assessment of hump crossings is limited. Based on an inspector's judgment, hump crossings are cataloged in a single field of the State's road inventory—a field which simply includes a yes or a no. Where crossings are assessed quantitatively (in Kentucky or elsewhere), a 2D approach is used (based on the road profile only, or, if based on a 3D pavement model, are still restricted to 2D for the vehicle). However, no methods exist to evaluate the potential impact of pavement cross section variation on all possible contact points of the vehicle and pavement. In part, the cost and difficulty of collecting 3D data has likely limited the development of tools for such analysis.

Today, 3D data are becoming widely available. Given a 3D point cloud, the distance between any two points of a crossing as well as and elevation differences between surfaces can be readily measured. Scenarios where vehicles with low ground clearance may become high-centered or hung-up on a crossing may be determined based on vehicle dimensions such as wheel base length and clearance height. Not only may such an application of 3D technology identify hump crossings, it may also be possible to quantify the severity of potential interference (some trucks “drag” their loads across) and be used to proactively improve safety at crossings.

This report presents a method to quantify and evaluate the complex geospatial interaction between vehicles and crossings, and is organized as follows:

- The second section presents background including a discussion of current design guidelines for rail grade crossings, previous studies and applications of hump crossing identification and current research on and application of 3D data collection for rail grade crossings.
- The third section describes field test locations and data collection efforts
- The fourth section presents a detailed methodology for identifying and assessing hump crossings

- A fifth section details test results
- The sixth section provides a field validation of the hump crossing assessment methodology.
- The seventh and concluding section presents conclusions, advantages, limitations and future application of the proposed methodology.

SECTION 2. BACKGROUND

Crossing geometric design guidance is provided in AASHTO’s A Policy on Geometric Design of Highways and Streets (the Green book) (American Association of State Highway and Transportation Officials (AASHTO), 2011), US DOT Railroad-Highway Grade Crossing Handbook (US Department of Transportation, 2007) and American Railway Engineering and Maintenance-of-Way Association (AREMA) Manual for Railway Engineering (American Railway Engineering Maintenance-of-Way Association (AREMA), 2015). These guides indicate that the surface of the highway should be neither more than 3 inches higher nor more than 6 inches lower than the top of the nearest rail at a point 30 feet from the rail, measured at a right angle, unless track superelevation dictates otherwise, as shown in Figure 2.1. Following these guidelines would prevent most all but the most extreme low and long vehicles from becoming hi-centered.

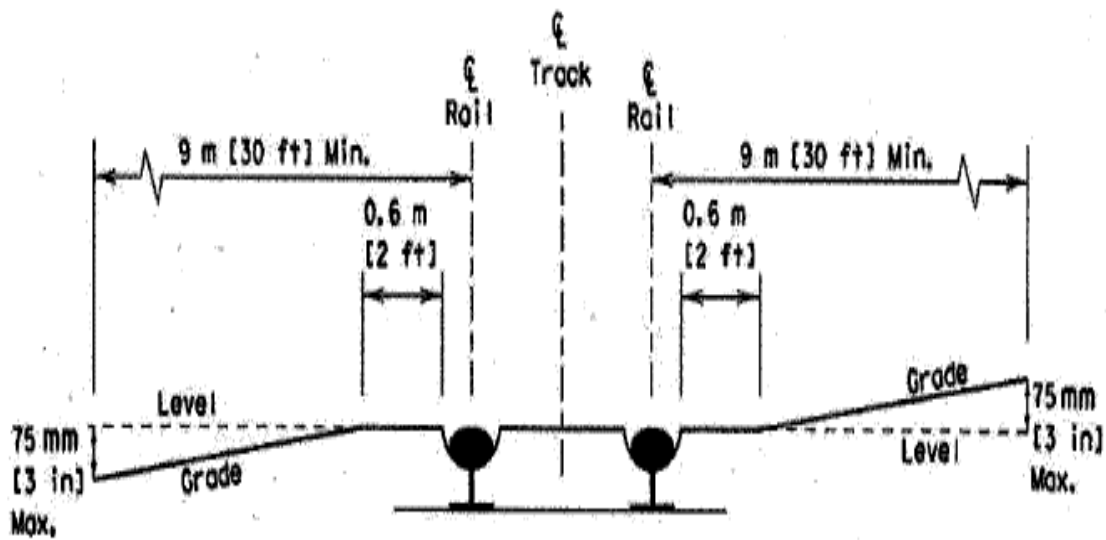


Figure 2.1 Rail-Highway grade crossing vertical alignment (AASHTO, 2011).

Previous efforts have been made to address the hump crossing issue. The “HANG-UP” software (Eck & Kang, 1992; Kang & Eck, 1991), developed in the early 1990s and later, related papers, (French, Clawson, & Eck, 2003) (Clawson, 2002), approach the hump crossing problem based

on two dimensional geometric design. These dimensions include only the vehicle length and clearance as well as the crossing profile to identify conflict points. These solutions do not consider that actual field crossings vary in cross section due to highway or rail superelevation, construction abnormalities or conditions such as rutting or potholes. Wheel paths may incur different profiles, not to mention that pavement may vary between wheel paths where most conflicts are likely to occur (e.g, in the center of the wheels at the low part of axle or between front and rear wheels and again in the middle of the wheel path.) Also, previous work has examined only a very sparse grid of potential conflict points (e.g., every five feet) and computing power limited the extension of the application into three dimensions.

Another approach to the identification of hump crossings has been to build physical models with frame and wheels and “drive” the model over crossings. Obviously, the physical model must be taken to each crossing and traffic control must be provided to conduct systematic evaluation. Such an evaluation is time consuming. Two additional disadvantages to the physical model approach are 1) the frame only represents a particular vehicle that may or may not be in the mix of vehicles that actually use the crossing, and 2) to assess the third dimension (cross section) of the crossing, the frame must be driven across the crossing multiple times.

Today, with the advent of low-cost and ubiquitous 3D technology and data (Wang, Souleyrette, Lau, & Xu, 2014), there are more analytical possibilities. Data collected by these methods provide the basis for a modeling crossings, and when combined with 3D models of design vehicles, facilitate investigating potential conflicts in three dimensions for any hump crossing.

SECTION 3. ACQUISITION 3D DATA OF CROSSING PAVEMENT

To develop and test the analytical methods proposed, data were collected for three crossings in Kentucky. These particular crossings were selected as representative of varying surface conditions, as-built profiles and single and double tracks.

For each of these, aerial imagery, LiDAR point clouds, and centerline profiles are visualized in Figure 3.1 through Figure 3.9.



Figure 3.1 Crossing A: Bryan Station Road (USDOT #346839X) aerial photo.

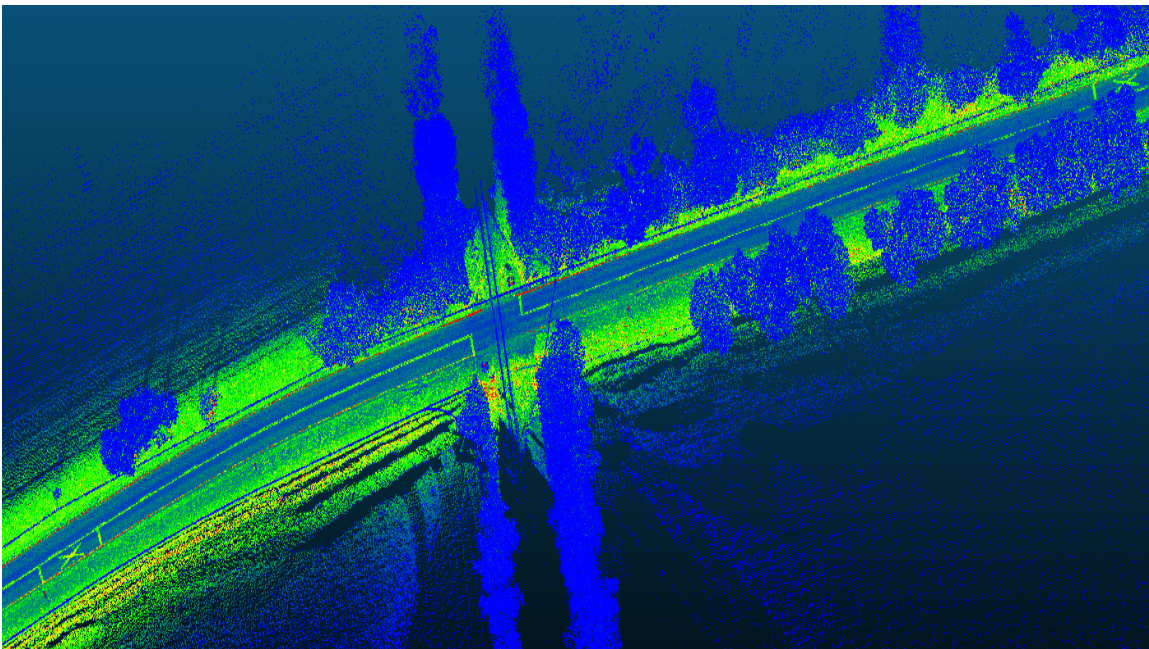


Figure 3.2 Crossing A: Bryan Station Road LiDAR point cloud.

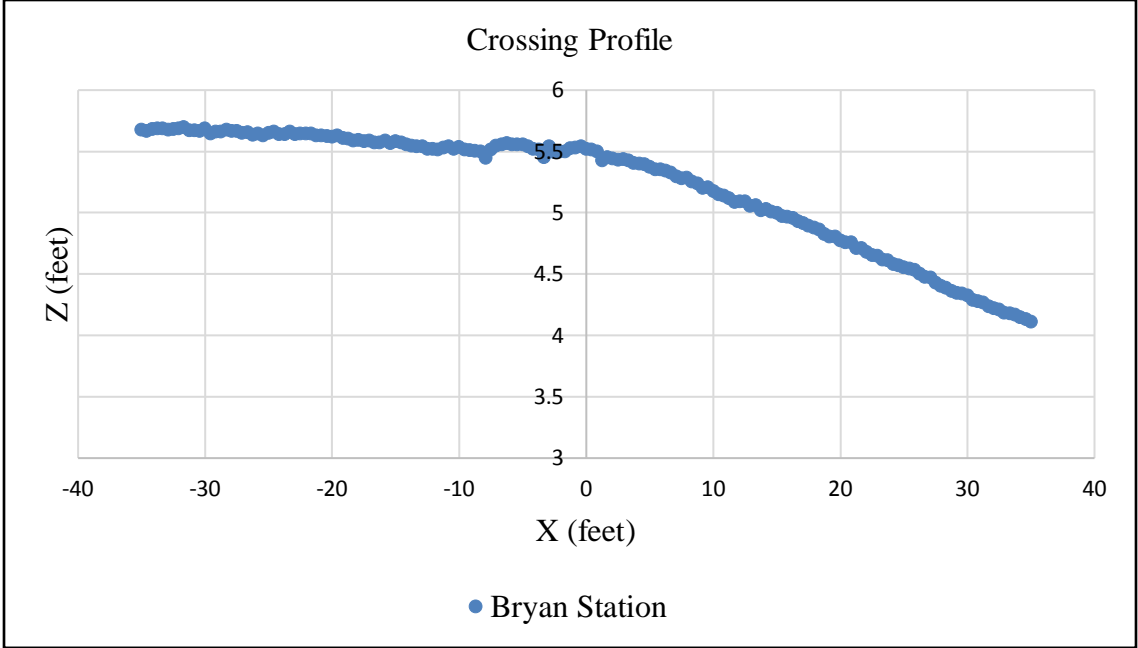


Figure 3.3 Crossing A: Bryan Station Road centerline profile.



Figure 3.4 Crossing B. Brannon Road crossing (USDOT # 841647U) aerial photo.

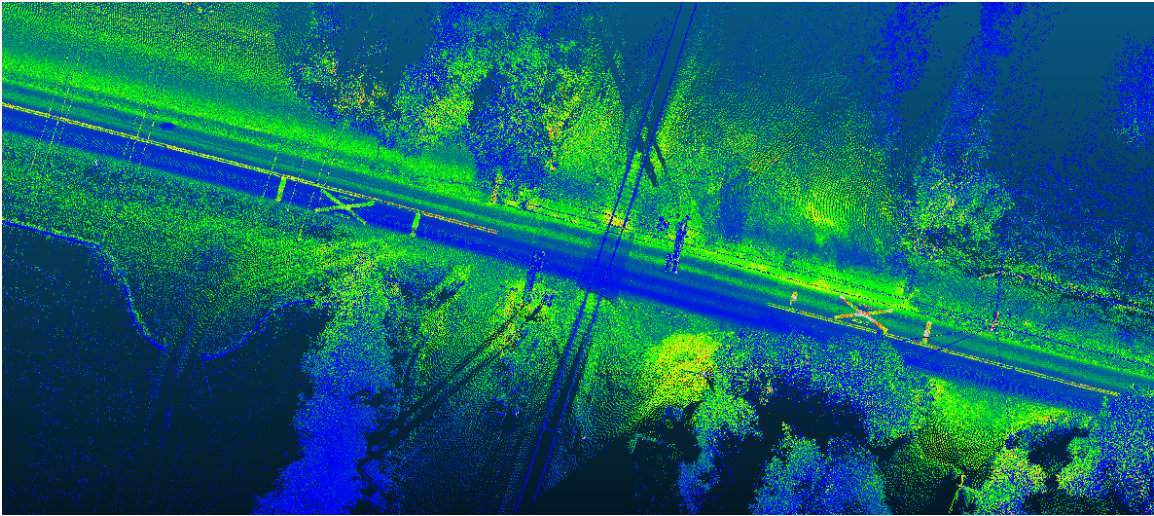


Figure 3.5 Crossing B. Brannon Road crossing LiDAR point cloud.

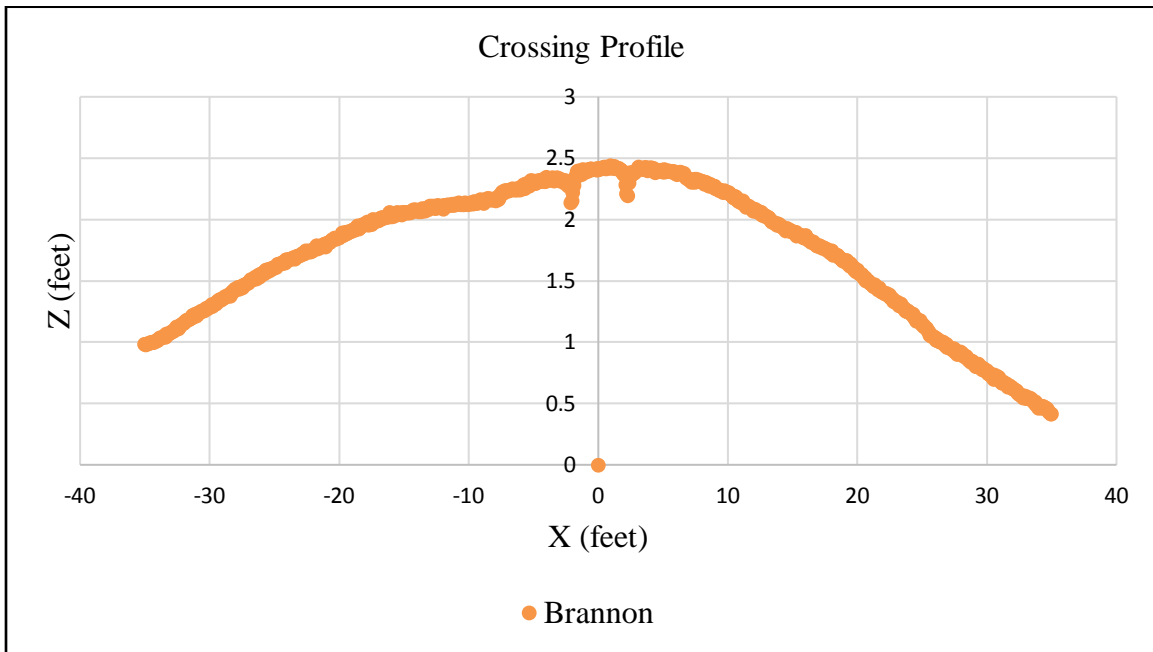


Figure 3.6 Crossing B. Brannon Road crossing centerline profile.



Figure 3.7 Crossing C. Briar Hill Road Army Depot Road crossing (USDOT # 346849D) aerial photo.

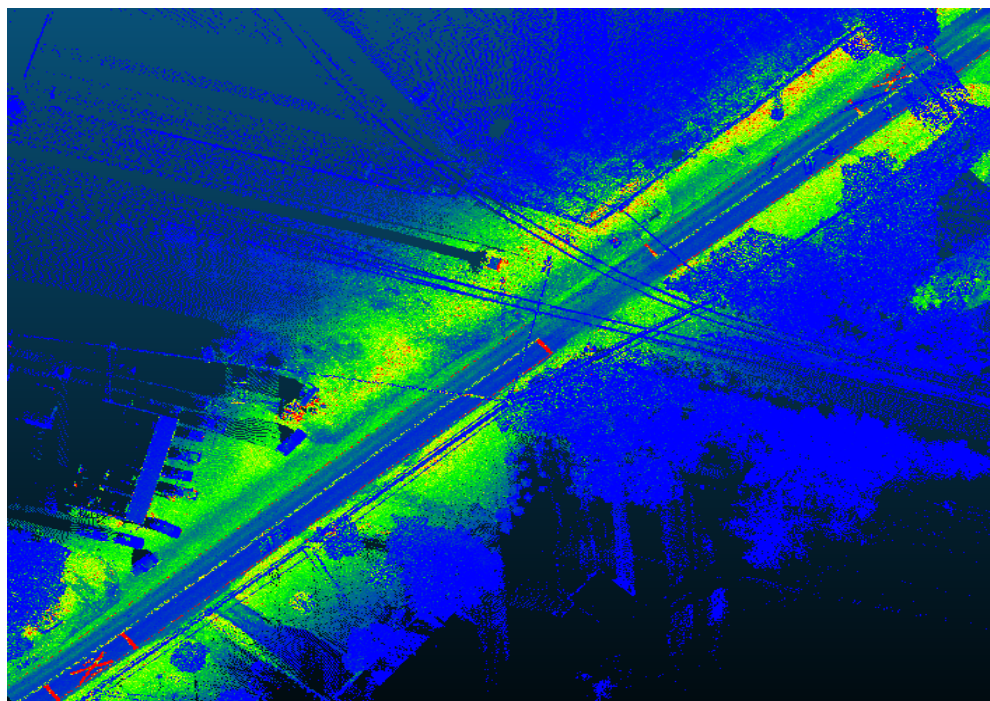


Figure 3.8 Crossing C. Briar Hill Army Depot Road crossing LiDAR point cloud

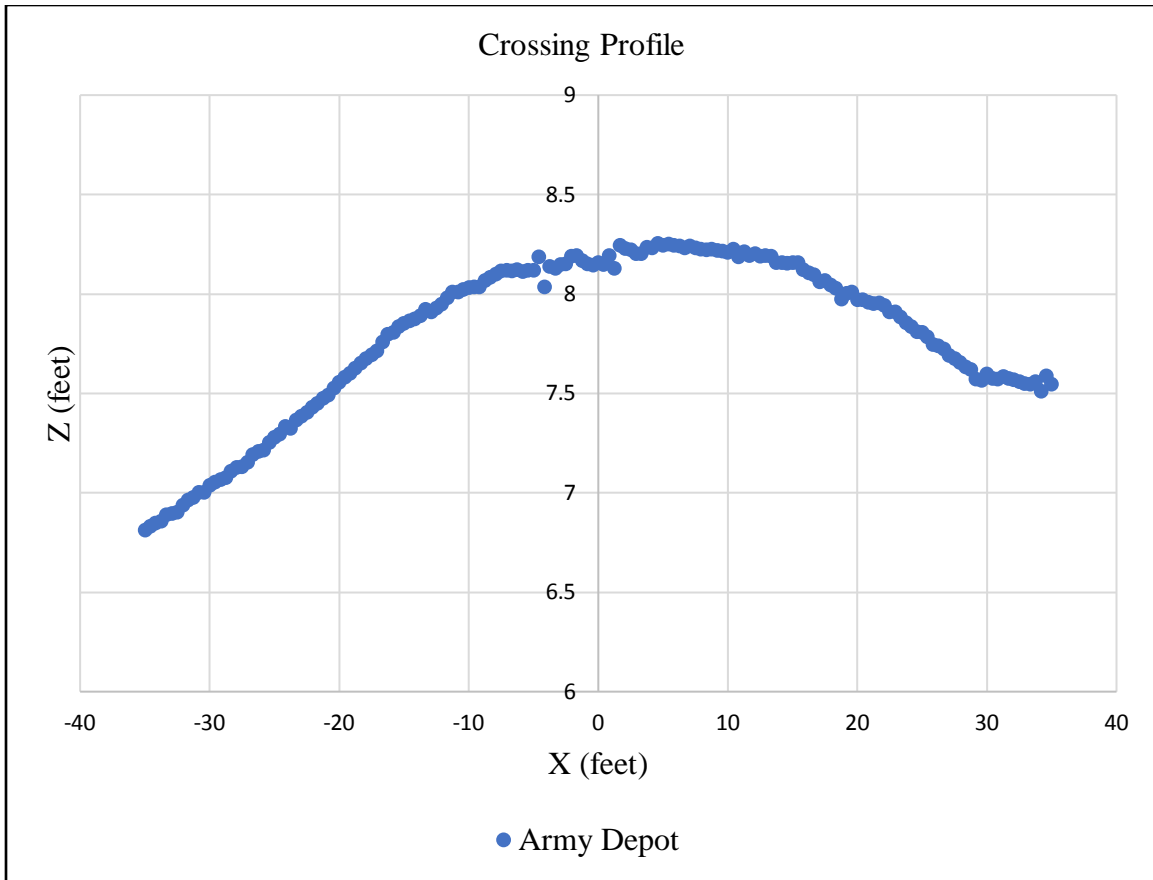


Figure 3.9 Crossing C. Briar Hill Army Depot Road crossing centerline profile.

SECTION 4. METHODOLOGY FOR QUANTIFYING RAIL-HIGHWAY HUMP CROSSINGS

In this section, a novel method is developed to quantify rail-highway hump crossings using 3D data. To facilitate the explanation of the methodology and to establish a reference framework, conditions and assumptions are listed below:

1. The origin of the local coordinate system (center of the crossing) is set as the intersection of the highway and railroad centerlines (center of the two tracks if double-track). The X-axis refers to the highway centerline. (See Figure 4.1)
2. The highway portion of the crossing is straight and analysis of approach is limited to 120 feet in each direction of the highway.
3. The railroad portion of the crossing is limited to the width of the highway.
4. Vehicle are considered as a rigid frame with 4 wheels. No flexible suspension is accounted for. Generally, only three of the four wheels will be in contact with the ground for an uneven surface (consider a table with four legs resting on an irregular surface).

5. The dimensions of vehicle wheel base, track width, front overhang, rear overhang and corresponding ground clearance are shown in Figure 4.2 and Table 4-1. The left front wheel is referred to as the number one wheel. The reference numbers for the other wheels and a local coordinate system for the vehicle are shown in Figure 4.2.
6. There are no deformation of the vehicle tire, frame or suspension, and so the worse-case condition is considered (at crawl speed). The frame bottom is considered to be formed by 3 plates, corresponding to the front overhang, area between the wheels and rear overhang.
7. Road pavement is considered as rigid (no appreciable deformation of the road under load).
8. The surface of the crossing is referenced on a 5×5 inch grid to reduce the density of the point cloud as well as number of calculations. Vehicle wheels are considered to move along grid cells. Although the actual contact area between the tire and pavement (contact patch) varies according to tire design, materials and pressure, the contact patch is assumed to occupy, at a minimum, 25 square inches. A typical truck tire will contact much more than 25 square inches (e.g., a maximum 9000 pound wheel load at 100 psi occupies 90 square inches.) The 5x5 inch grid used in the analysis is quite conservative (the 5 inch patch will be sufficient to identify potholes or ruts that will affect vehicle placement).
9. There is no contact point between vehicle and pavement except wheels.
10. When a wheel contacts the pavement, it will contact the highest point measured within the grid block.

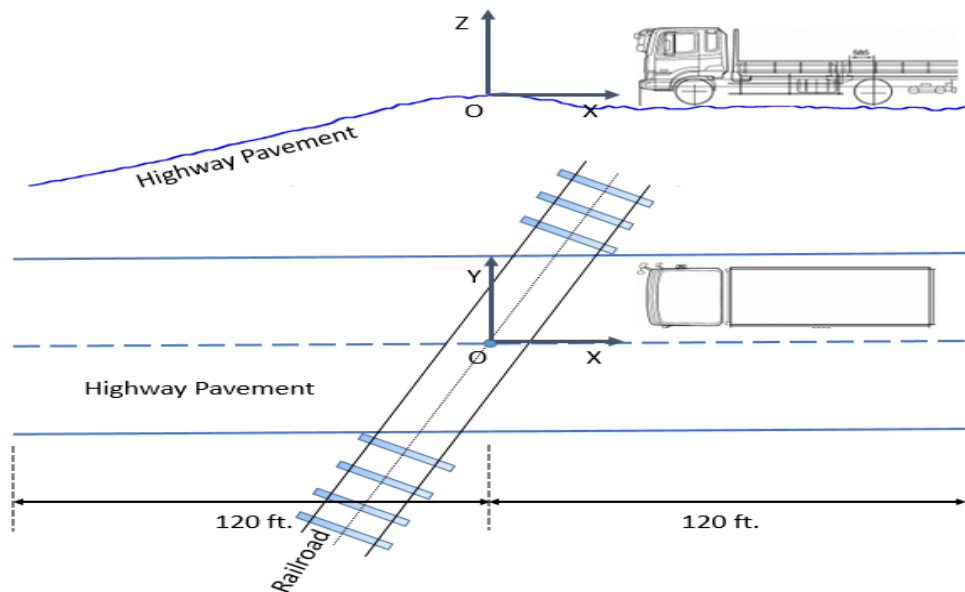


Figure 4.1 Hump crossing coordinate system (not to scale).

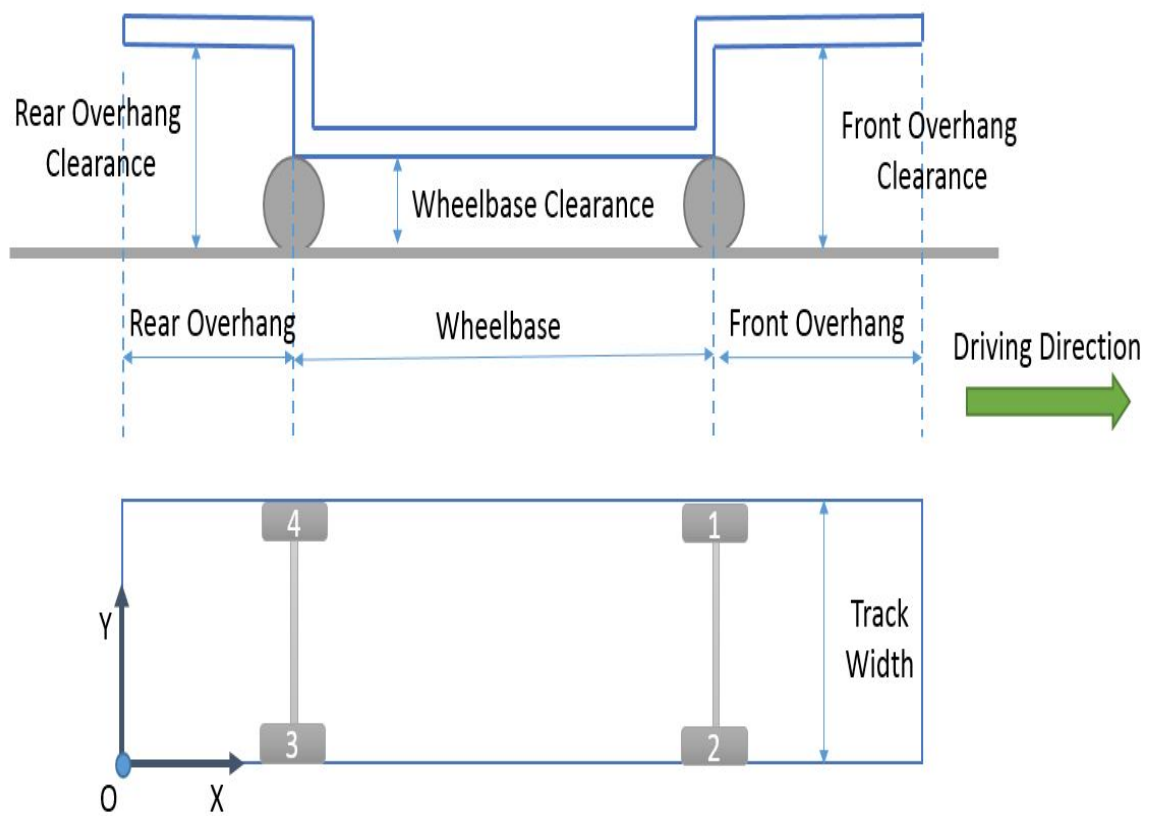


Figure 4.2 Vehicle model dimensions and coordinate system (not to scale).

Table 4-1 Parameters of typical low clearance vehicles

No.	Design Vehicle	Wheel base (ft)	Assumed Track Width (ft)	Front Overhang (ft)	Rear Overhang (ft)	Ground Clearance (inch)		
						Wheel base	Front Overhang	Rear Overhang
1	Rear-Load Garbage Truck	20	8.5	--	10.5	12	--	14
2	Aerial Fire Truck	20	8.5	7	12	9	11	10
3	Pumper Fire Truck	22	8.5	8	10	7	8	10
4	School Bus	23	8.5	--	13	7	--	11
5	Lowboy Trailers <53 feet	38	8.5	--	--	5	--	--
6	Car Carrier Trailer	40	8.5	--	14	4	--	6
7	Limousine	20	8.5	--	--	4	--	--

The basic approach of the methodology is to place specific vehicle models at every possible position on the highway portion of the crossing. At each position, the minimum elevation difference, δ_{min} , between vehicle base and highway pavement can be checked. If δ_{min} is greater than 0, there is no contact between the vehicle and pavement (assuming the vehicle is not bouncing). If δ_{min} is less than 0, conflict will occur. The minimum elevation difference, δ_{min} , and its position relative to both vehicle base and crossing are recorded to enable identification of worst conflict (highest elevation difference).

The analytical procedure is represented by the flowchart shown in Figure 4.3, which can be divided into three steps: preprocessing, processing and summarizing.

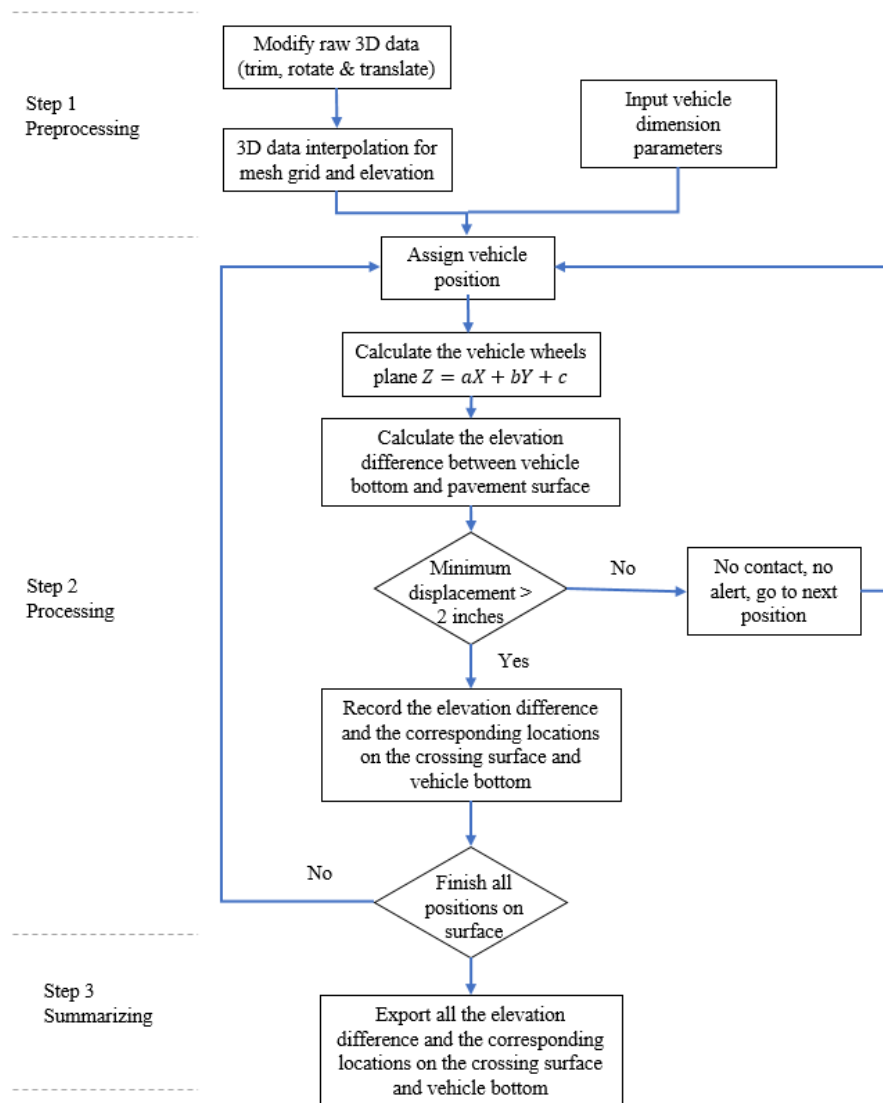


Figure 4.3 Analysis procedure flow chart.

In the first step, data are pre-processed. 3D raw data are trimmed, offset and rotated to align with the local coordinate system. Next, the point cloud is resampled and thinned to a 5×5 inch XY grid, producing surface P which is defined by a set of points P(i) with coordinates $(x_{P(i)}, y_{P(i)}, z_{P(i)})$ for all i where $i = 1, 2, \dots, n$, and n is the number of points comprising the surface. Preprocessed 3D data of for the KY-57 Briar Hill Army Depot Crossing is shown in Figure 4.4.

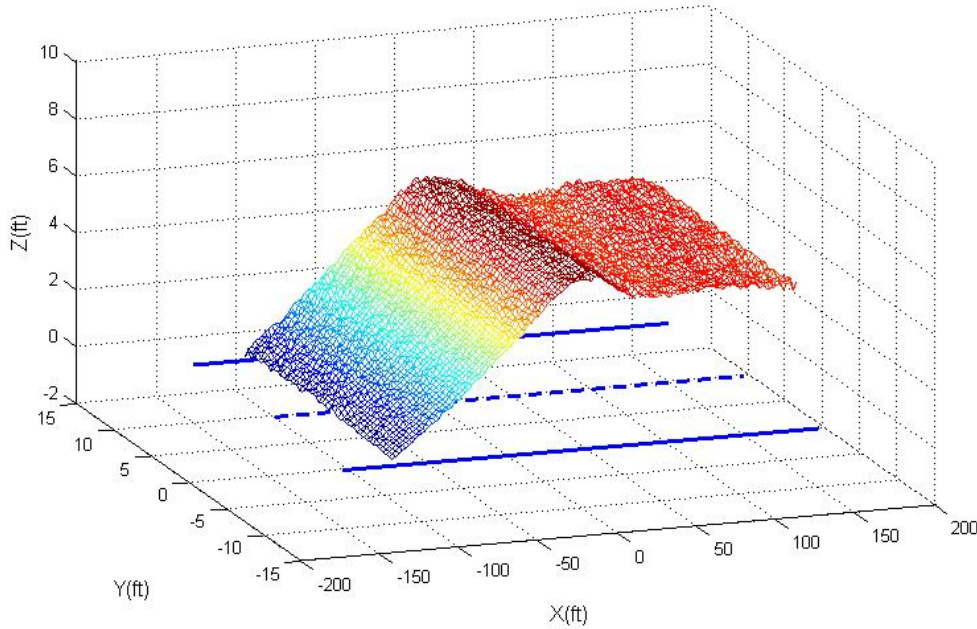


Figure 4.4 Preprocessed 3D data of KY-57 Briar Hill Army Depot crossing.

In the second step, a vehicle is “moved” to a location on the crossing surface. W can be defined as the set of points comprising the bottom of the wheels of the vehicle. Each wheel bottom $W(j)$ has coordinates $(x_{W(j)}, y_{W(j)}, z_{W(j)})$ for all $j=1-4$ (wheel order 1-4 as shown on Figure 4.2). For example, when wheel 1 is moved to the assigned position $P(1)$ with surface coordinates $x_{P(1)}, y_{P(1)}, z_{P(1)}$, the x, y position of all four wheels is defined as:

$$x_{W(1)} = x_{P(1)}, y_{W(1)} = y_{P(1)}; \quad x_{W(2)} = x_{P(1)}, y_{W(2)} = y_{P(1)} - t;$$

$$x_{W(3)} = x_{P(1)} - L, y_{W(3)} = y_{P(1)} - t; \quad x_{W(4)} = x_{P(1)} - L, y_{W(4)} = y_{P(1)}.$$

Where t is the track width and L is the wheel base length.

For the rigid frame vehicle models on an irregular surface, there are 4 wheel contact patterns to be evaluated:

- I. Wheel No. 2, 3 and 4;
- II. Wheel No. 1, 3 and 4;

III. Wheel No. 1, 2 and 4;

IV. Wheel No. 1, 2 and 3.

Take pattern I for example. At the initial x, y position of the vehicle wheels (shown above), the Z coordinates of wheels 2, 3 and 4 are simply the Z coordinates of the surface at these locations. These known points define a plane parallel to the vehicle base. The elevations of any plane can be expressed by the equation:

$$Z = aX + bY + c$$

Where a, b and c are undetermined coefficients. These coefficients can be solved for using a system of equations defined by three points:

$$a = \frac{\begin{vmatrix} z_2 & y_2 & 1 \\ z_3 & y_3 & 1 \\ z_4 & y_4 & 1 \end{vmatrix}}{\begin{vmatrix} x_2 & y_2 & 1 \\ x_3 & y_3 & 1 \\ x_4 & y_4 & 1 \end{vmatrix}} \quad b = \frac{\begin{vmatrix} x_2 & z_2 & 1 \\ x_3 & z_3 & 1 \\ x_4 & z_4 & 1 \end{vmatrix}}{\begin{vmatrix} x_2 & y_2 & 1 \\ x_3 & y_3 & 1 \\ x_4 & y_4 & 1 \end{vmatrix}} \quad c = \frac{\begin{vmatrix} x_2 & y_2 & z_2 \\ x_3 & y_3 & z_3 \\ x_4 & y_4 & z_4 \end{vmatrix}}{\begin{vmatrix} x_2 & y_2 & 1 \\ x_3 & y_3 & 1 \\ x_4 & y_4 & 1 \end{vmatrix}}$$

The z coordinate value of wheel No.1 can be calculated as:

$$z_{W(1)} = ax_{W(1)} + by_{W(1)} + c .$$

- If $z_{W(1)} \geq z_{P(i)} [at\ x(W1),y(W1)]$, wheel 1 is above the pavement. Patterns I and III are practical cases where this may occur.
- If $z_1 < z_{P(i)} [at\ x(W1),y(W1)]$, wheel 1 is under the pavement. Therefore, only patterns II and IV are practical.

For the practical pattern combinations, the elevation difference δ between vehicle and crossing can be calculated for all points on the vehicle underbody surfaces.

$$z(\text{vehicle}) = ax + by + c + Clearance_{Front\ overhang} \quad (x,y) \in A_{front\ overhang}$$

$$z(\text{vehicle}) = ax + by + c + Clearance_{Wheelbase\ area} \quad (x,y) \in A_{wheelbase\ area}$$

$$z(\text{vehicle}) = ax + by + c + Clearance_{rear\ overhang} \quad (x,y) \in A_{rear\ overhang}$$

$$\delta = z(\text{vehicle}) - z(\text{crossing surface}), \text{ for all vehicle underbody surface points}$$

If $\delta_{min} < 0$, the vehicle will contact the pavement. For safety considerations, a minimum difference can be set as a warning value. If δ_{min} is less than the warning value, the corresponding position on both vehicle underbody and crossing pavement can be recorded.

The second step is then repeated for all possible vehicle positions along the crossing surface for both directions over the crossing. In the third step of the methodology, elevation differences are recorded and exported to a file for all crossing/vehicle underbody point combinations.

A MATLAB program was developed to implement and test the methodology described above. A typical car carrier trailer was selected as a test vehicle. For this vehicle, the wheelbase is 40 feet with a clearance of 6 inches. Its length of rear overhang is 14 feet with clearance of 4 inches. Figure 4.6 shows the results if the trailer passed the KY-57 Briar Hill army depot crossing. The top part of the figure present a plot of contact points referenced to the local crossing coordinate system. The dotted line in the plot represents the centerline of the road. The lower portion of the figure shows a plot of contact position on the underside of the vehicle. Severity of conflict (difference in elevation) is represented by color. Conflicts occurred both under the wheelbase and under the rear overhang. When the two axles of the truck are on the opposite sides of the crossing, wheelbase contact may occur. In this situation, $\delta_{min} = -4.91$ inch, at a point located to the north of the crossing near the railroad. Rear overhang conflict occurs when the front axle approaches the railroad. The front of the vehicle will rise causing the rear overhang to scrape the ground. In this situation $\delta_{min} = -2.99$ inch.



Figure 4.5 Car carrier trailer.

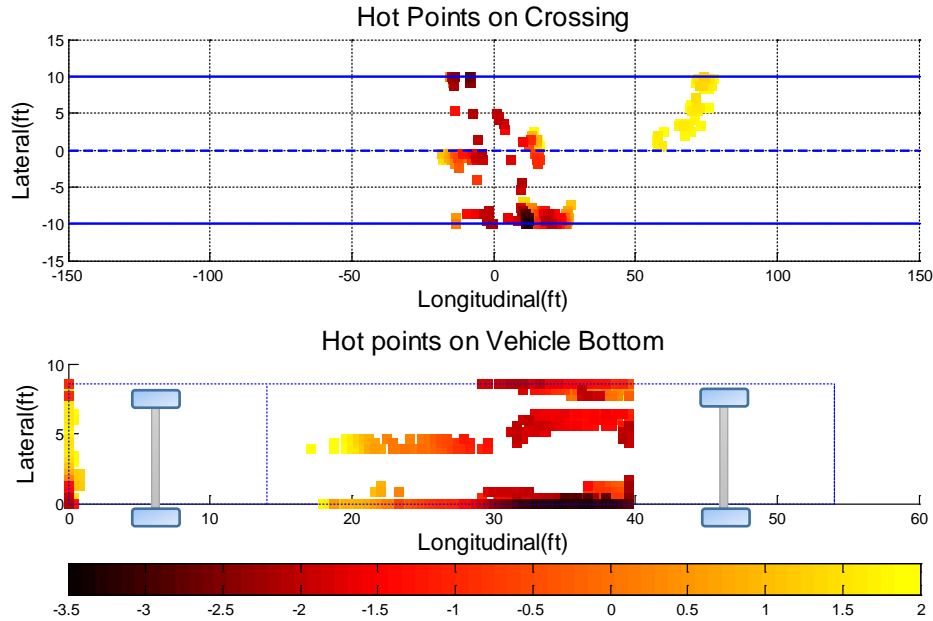


Figure 4.6 Car carrier trailer contact points at KY-57 Briar Hill Army Depot crossing.

SECTION 5. ANALYSIS AND RESULTS

For all three study crossings, seven vehicle types were selected for analysis, as shown in Table 5-1. Although many types of vehicles may use a particular crossing, it would be time consuming to assess all possible passing vehicles. Vehicles 1 through 5 are common for these crossings, where numbers 6 and 7 are less commonly seen on the types of highways.

The minimum distance δ_{min} represent the severity of humping. If δ_{min} is only slightly smaller than zero, the flexibility of the vehicle body and its suspension system may enable the vehicle to pass, perhaps only scraping the surface of crossing. However, if δ_{min} is much smaller, the vehicle may become stuck. Correspondingly, a five-level evaluation criterion is proposed:

Level 1: $\delta_{min} > 2$ inch

Level 2: $2 \text{ inch} \geq \delta_{min} > 0 \text{ inch}$

Level 3: $0 \text{ inch} \geq \delta_{min} > -1 \text{ inch}$

Level 4: $-1 \text{ inch} \geq \delta_{min} > -2 \text{ inch}$

Level 5: $\delta_{min} \leq -2 \text{ inch}$

Results for the crossings are presented in Table 7-2. Observations include:

1. Vehicle type 1 may safely negotiate all crossings

2. Vehicle types 2, 3, 5, and 7 crossings A and C are characterized mainly by L1 or L2 conflict (no contact), but for crossing B, some contact will be made front and/or rear overhangs.
3. Vehicle types 5 and 6 will have seriously problems negotiating all three crossings.

Table 5-1 Evaluation of Railroad – Highway crossing

Veh. type	KY-57 Bryan Station (A)			Brannon Rd (B)			KY-57 Briar Hill Army Depot (C)		
	Wheel base	Front Over hang	Rear Over hang	Wheel base	Front Over hang	Rear Over hang	Wheel base	Front Over hang	Rear Over hang
1	L1	-	L1.	L1	-	L1	L1.	-	L1
2	L1	L1	L1	L1	L1	L5	L1	L1	L1
3	L1	L1	L1	L2	L3	L4	L1	L1	L1
4	L1	-	L1	L2	-	L3	L1	-	L1
5	L3	-	-	L5	-	-	L4	-	-
6	L4	-	L1	L5	-	L5	L5	-	L3
7	L2	-	-	L4	-	-	L2	-	-

Figure 5.1 through Figure 5.3 depict contact points for the three crossings. The minimum values of elevation difference between vehicles and crossings are (-3.5) inches, (-7.0) inches and (-5.0) inches, respectively. According to these data, all can be considered to be hump crossings, while crossing B is most severe.

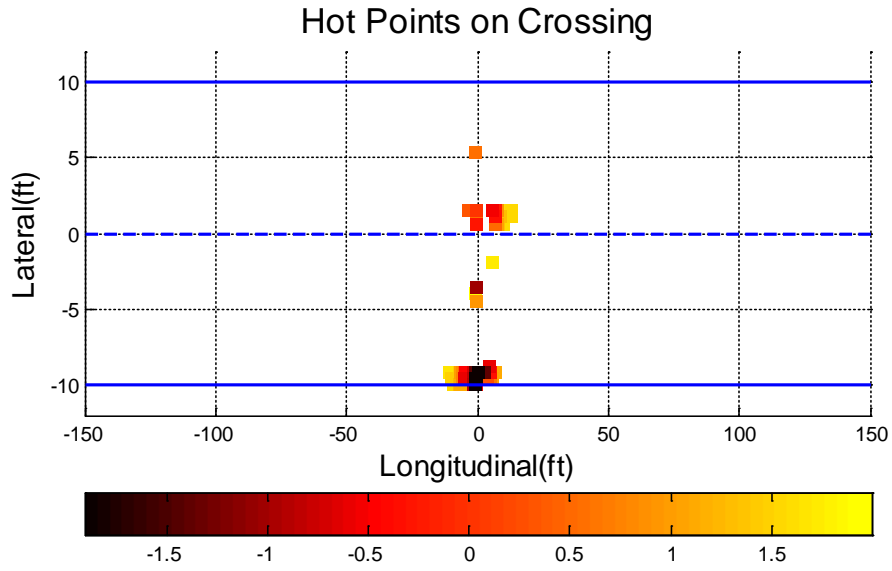


Figure 5.1 Contact points on KY-57 Bryan Station crossing (A)

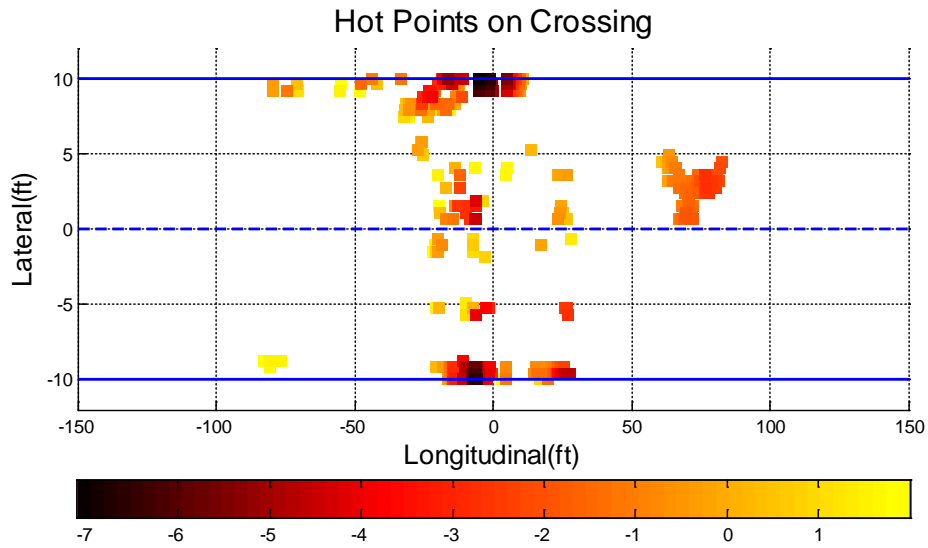


Figure 5.2 Contact points on Brannon Rd crossing (B)

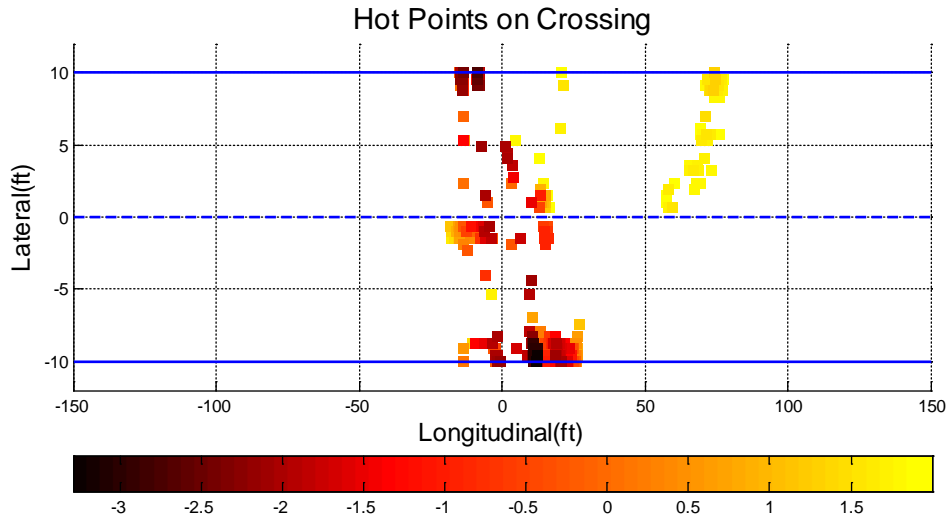


Figure 5.3 Contact points on KY-57 Briar Hill Army Depot (C)

SECTION 6. VERIFICATION

After completing the analysis and examining the results, several field verification visits were conducted. In the field, a survey tape and level rods were used to measure elevations along the crossing. Different vehicle clearances were marked on the rods which were connected by tape to build a physical model. This model was used to sweep over the crossing surface from left to right and check for contact points as shown in Figure 6.1 and Figure 6.2. Scraping marks on the crossing pavement were compared with conflict maps. The verification concluded that while there was a correlation between modeled and observed conflicts (scrape marks), not all areas indicated by the methodology had scrape marks. This is likely due to the absence of some of the vehicle types at the actual locations, vehicle characteristic that are not similar to the ones used in the analysis, or deterioration of previous marks due to weathering. See Figure 6.3 and Figure 6.4.



Figure 6.1 Field verification A.



Figure 6.2 Field verification B.



Figure 6.3 Crossing scratch marks A.



Figure 6.4 Crossing scratch marks B.

SECTION 7. CONCLUSION AND RECOMMENDATIONS

This research presented the development and testing of a methodology to identify and quantify the potential severity of hump crossings. Results indicate promise for the use of 3D datasets to improve systems inventories and reduce potential risks of highway-rail collisions due to vehicles becoming stuck at crossings. With the proposed methodology, all possible contact areas between vehicle undersides and crossings can be investigated. The method provides a far richer database to road managers than a simple yes/no inventory. Warning areas are identified and can be customized to any vehicle with known geometry. Once a crossing 3D point cloud is obtained, any vehicle and any wheel path can be simulated to provide results without the need for field visits and concomitant risks. Of course, the practical application of such a methodology depends on the availability of 3D data. Future work could be to investigate the impact of dynamic forces on hump crossing conflict (Wang, Souleyrette, Aboubakr, & Lau, 2015), incorporating aspects such as speed and suspension into the model.

REFERENCES

- American Association of State Highway and Transportation Officials (AASHTO). (2011). *A Policy on geometric design of highways and streets 2011* (6th ed.). Washington DC.
- American Railway Engineering Maintenance-of-Way Association (AREMA). (2015). *2015 manual for railway engineering*.
- Bauer, L. (1958). Passenger car overhang and underclearance as related to driveway profile design. II. Street and highway design. *Highway Research Board bulletin, 195*, 23-29.
- Clawson, A. L. (2002). *Establishing Design Vehicles for the Hang-up Problem*: West Virginia University Libraries.
- Eck, R. W., & Kang, S. (1992). Roadway Design Standards to Accommodate Low-Clearance Vehicles *Transportation Research Record*(1356).
- French, L., Clawson, A., & Eck, R. (2003). Development of design vehicles for hang-up problem. *Transportation Research Record: Journal of the Transportation Research Board*(1847), 11-19.
- Kang, S., & Eck, R. W. (1991). Low-Clearance Vehicles at Rail-Highway Grade Crossings: An Overview of the Problem and Potential Solutions. *Transportation Research Record*(1327).
- StudioNoeProductions. (2015). Amazing Limo vs Train Crash Elkhart County [Video file]. Retrieved from <https://youtu.be/Ss8RdZLPCvs>
- US Department of Transportation, Federal Highway Administration. (2007). *Railroad-Highway Grade Crossing Handbook*.
- Wang, T., Souleyrette, R. R., Aboubakr, A. K., & Lau, D. (2015). A Dynamic Model for Quantifying Rail-Highway Grade Crossing Roughness. *Journal of Transportation Safety & Security*, 00-00. doi:10.1080/19439962.2015.1048016
- Wang, T., Souleyrette, R. R., Lau, D., & Xu, P. (2014). *Rail Highway Grade Crossing Roughness Quantitative Measurement Using 3D Technology*. Paper presented at the 2014 Joint Rail Conference. <http://dx.doi.org/10.1115/jrc2014-3778>